Comparative analysis of synthetic GNSS time series - Bias and precision of velocity estimations

Stephane Mazzotti, Aline Déprez, Eric Henrion, Christine Masson, Frédéric Masson, Jean-Luc Menut, Marianne Métois, Jean Matthieu Nocquet, Lucie Rolland, Pierre Sakic, et al.

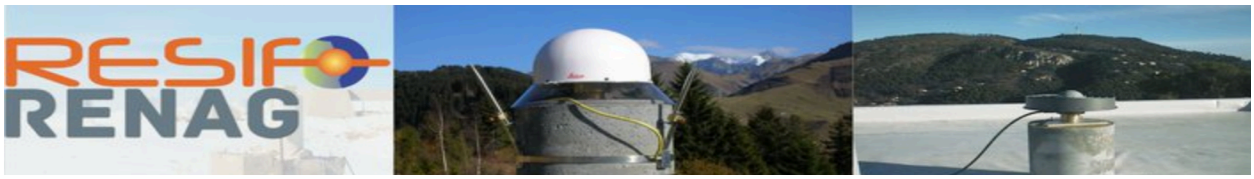

RENAG - RESIF Report

Comparative analysis of synthetic GNSS time series - Bias and precision of velocity estimations

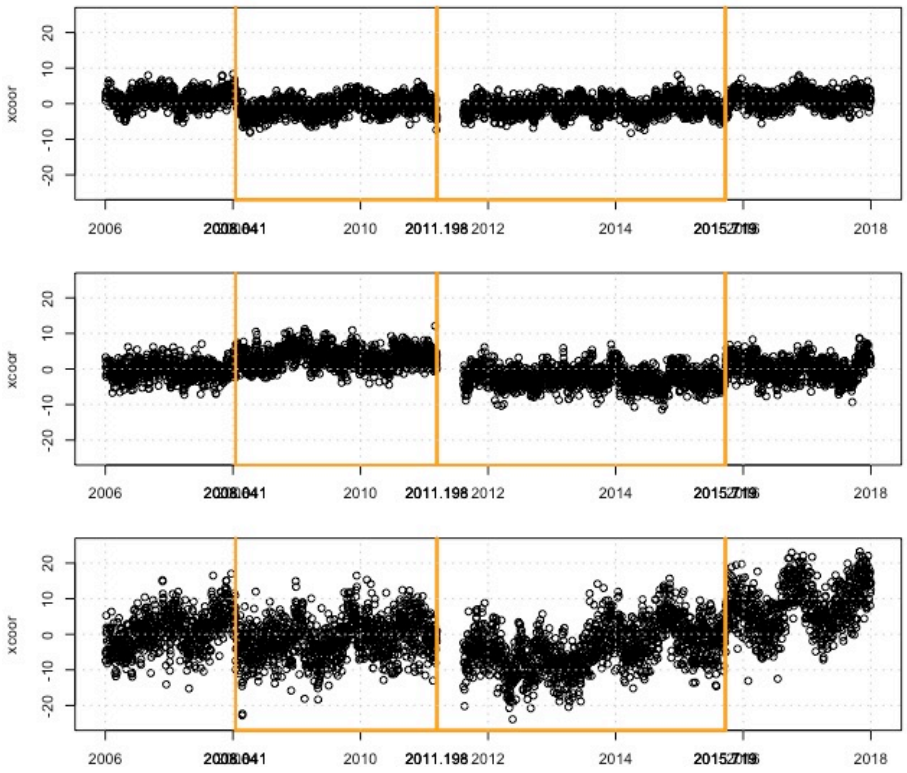

RENAG/RESIF est soutenu par les Investissements d'Avenir (projet RESIF-CORE)

Comparative analysis of synthetic GNSS time series - Bias and precision of velocity estimations

Stephane Mazzotti [1], Aline Deprez [2], Eric Henrion [3], Christine Masson [1], Frédéric Masson [3], Jean-Luc Menut [4], Marianne Métois [5], Jean-Matthieu Nocquet [4, 6], Lucie Rolland [4], Pierre Sakic [7], Anne Socquet [2], Alvaro Santamaría-Gómez [8], Pierre Valty [9], Mathilde Vergnole [4], Philippe Vernant [1]

1. Géosciences Montpellier (GM), UMR 5243, Université de Montpellier, CNRS. Place E. Bataillon, 34095 Montpellier cedex, France.

2. Institut des Sciences de la Terre (ISTerre), UGA, CNRS, USMB, IRD, IFSTTAR. 38058 Grenoble Cedex 9, France.

3. Institut de Physique du Globe, UMR7516, Université de Strasbourg/EOST, CNRS. 5 rue René Descartes, F-67084 Strasbourg Cedex, France.

4. Géoazur, Université Côte d'Azur, CNRS, Observatoire de la Côte d'Azur, IRD. 250 rue Albert Einstein, Sophia Antipolis, 06560 Valbonne, France.

5. Laboratoire de Géologie de Lyon (LGTPE), Université Claude Bernard Lyon 1, bat. Géode, 69100 Villeurbane, France.

6. Institut de Physique du Globe Paris. 1 rue Jussieu, 75238 Paris cedex 05, France.

7. Helmholtz-Zentrum, GeoForschungsZentrum. Telegrafenberg (GFZ), D-14473 Potsdam, Germany.

8. GET, Université de Toulouse, CNES, CNRS, IRD, UPS. Toulouse, France.

9. Service de géodésie et nivellement, IGN. 73, Av. de Paris, 94160 Saint Mande, France.

This report summarizes the analyses carried out between February 2018 and June 2019 within the RENAG consortium (Réseau National GNSS, http://renag.resif.fr), part of the RESIF research infrastructure (French Seismologic and Geodetic Network, https://www.resif.fr). The project was implemented as an internal exercise designed to assess the variability in GNSS time series analyses and derived velocities for the RENAG-RESIF stations.

Synthetic time series creations, statistical analyses of solutions, and figures were done using the R software (R Core Team, 2016).

Summary

105 synthetic time series replicating GNSS 3D position series are analyzed independently by nine different groups within the RENAG consortium in order to characterize the variability in estimations of long-term velocities. The main objective is not a detailed study of the parameters and sources controlling velocity variations, but simply to establish first-order conclusions regarding the uncertainties on GNSS velocity estimations as a function of the different analysis methods and software. Because the true velocities are known, our results are presented in terms of **velocity biases** (i.e. deviations of the estimated velocities relative to the expected values). Statistics on these biases can then be used as indicators of the potential precision of actual GNSS velocities.

To first order, the nine methods and software of time series analysis provide horizontal (resp. vertical) velocity estimations at precisions better than 1.0 mm/a (resp. 2.0 mm/a). None of the tested methods or software clearly stands out as significantly better or worse than the others. However, a group of four solutions (including the unweighted average of all nine solutions) provides systematically better results than the others. They are based on a standard time series analysis using a least-square inversion of a parametric model (velocity, seasonal terms, offsets) with either automatic and manual offset detection methods.

For time series with noise and duration characteristics corresponding to classical GNSS data (e.g., RENAG-RESIF stations), the velocity biases (and thus potential GNSS velocity precision) are characterized by the following statistics:

- Medians ca. 0.1 mm/a (horizontal components) and 0.1–0.3 mm/a (vertical component).
- 95th percentiles ca. 0.2–0.7 mm/a (horizontal components) and 0.5–2.0 mm/a (vertical component).
- RMS (root-mean-square) ca. 0.1–0.3 mm/a (horizontal components) and 0.3–0.9 mm/a (vertical component).

In addition to the variability of velocity estimations as a function of the analysis methods, first order information can be derived regarding the solution combination and velocity uncertainties:

- The unweighted average of all nine analyses yields results systematically in the upper tier of all individual solutions.
- Formal velocity uncertainties (standard errors) calculated on the basis of colored-noise models are statically representative of the velocity biases.
- In contrast, formal velocity uncertainties (standard errors) calculated using other methods (white noise or statistical variance) are not representative of the velocity biases (resp. significantly too low or too high).

1) Synthetic data description

Synthetic position time series are generated for a set of 35 stations grouped in 5 categories representing the spectrum of actual GNSS series characteristics (noise level, number of offsets, completeness). From the highest to the lowest quality, the five groups are: "SC" (Super Clean, stations SC01–SC07); "RC" (Rather Clean, stations RC01–RC07); "MR" (Mid Range, stations MR01–MR07); "RU" (Rather Ugly, stations RU01–RU07); "SU" (Super Ugly, stations SU01–SU07). The long-term velocities (cf. eq. 1) range between -2 and +2 mm/a, with the majority ca. -0.5 – +0.5 mm/a, in order to represent the relative velocities between stations in France and Western Europe (i.e., intraplate velocities in a local reference frame such as those measured by RENAG-RESIF stations).

NB: Stations in the SU group correspond to rare cases of extreme noise levels and are not representative of standard GNSS series used in geodetic studies. They are provided for information but are not included in the results and conclusions.

For each station, three daily position time series *x(t)* are generated to represent the North, East and Up components:

$$x(t) = x_0 + vt + A_1 sin(\omega_1 t + \phi_1) + A_2 sin(\omega_2 t + \phi_2) + B_i H(t, T_i) + \varepsilon(t, \kappa, C) \qquad (1)$$

with x_0: intercept of the position series; v: linear velocity; ω_1 and ω_2: periods of the annual and semi-annual signals; A_1 and A_2: amplitudes of the annual and semi-annual signals; B_i and T_i: amplitude and date of the ith offset expressed as a Heaviside function:

$$H(t, T_i) = 0\ , t < T_i\ ;\ H(t, T_i) = 1\ , t \geq T_i \qquad (2)$$

The offset dates T_i are identical for the three components but the amplitudes B_i can vary between each component. A random daily dispersion $\varepsilon(t, \kappa, C)$ is added to each series following a colored-noise model (*Kasdin, 1995*), with κ and C the spectral index and amplitude (expressed as the daily RMS _ Root-Mean-Square) of the dispersion. The annual and semi-annual phases (ϕ_1 and ϕ_2) are randomly generated for each series. The parameter values are given in Table 1.

For each quality group, synthetic series are produced for durations of 10–12, 19 and 29 years (resp., 2 or 3 stations, 2 or 3 stations, 2 stations). These durations are chosen to represent standard GNSS data used in geodynamic studies (10–20 years), plus prolonged data allowing testing the impact on velocity estimations of an extra 10 years of data.

The method to detect and manage offsets is a critical element of GNSS time series analysis and velocity estimation (*Gazeau et al., 2013; Masson et al., 2019*). Our objective is not a detailed study of this effect but only to provide sets of results representative of actual GNSS data. In order to include offset management as a study parameter, each station is accompanied by a pseudo "log file" comprising dates of "equipment changes". These dates correspond partly to actual offsets imposed in the series and partly to "false alarms" (i.e., dates with no imposed offset). In addition, some of the imposed offsets are not included in the log files.

The position time series for the 35 stations are shown in Appendix 1. The full dataset comprises, for each station, text files with positions and dates, pseudo logs, true parameter values (velocities, offset dates and amplitudes). It is available in the archive accompanying this report and upon request to the authors.

NB: The true parameter values were not transmitted to the analysis groups during the processing phase.

Table 1. Time series parameters of the 5 station categories

		Super Clean	Rather Clean	Mid Range	Rather Ugly	Super Ugly
completeness (% of available days)		98	95	90	80	70
κ		-0.30	-0.50	-0.70	-0.90	-1.10
C (mm)	**N**	1.8	2.0	2.2	2.8	3.9
	E	2.2	2.6	2.7	3.5	5.0
	U	4.0	4.9	5.3	7.0	8.0
A1 (mm)	**N**	1.0	1.0	1.0	1.0	1.0
	E	1.0	1.0	1.0	1.0	1.0
	U	3.0	3.0	3.0	3.0	3.0
A2 (mm)	**N**	0.5	0.5	0.5	0.5	0.5
	E	0.5	0.5	0.5	0.5	0.5
	U	1.0	1.0	1.0	1.0	1.0
number of offsets		0 - 2	1 - 3	1 - 4	2 - 4	3 - 5

2) Time series analysis methods and software

The synthetic time series are analyzed independently by different laboratories and research departments of the RENAG consortium using various software and methods, yielding nine independent solutions:

- **S1** - MIDAS software (*Blewitt et al., 2016*). Automatic velocity and uncertainty estimations based statistical analysis of position couples over one-year spread. No offset detection or estimation. Data analysis: A. Deprez, A. Socquet, ISTerre. [1]
- **S2** - homemade software (MATLAB based). Least-square inversion of parametric model (eq. 1), uncertainties computed using CATS software (*Williams, 2008*). Offsets imposed based on manual detection. Data analysis: E. Henrion, EOST.
- **S3** - homemade software (R based). Least-square inversion of parametric model (eq. 1), uncertainties computed with colored-noise approximation. Automatic detection + manual verification of offsets. Data analysis: C. Masson, GM.
- **S4** - software developed at INGV, Roma. Least-square inversion of parametric model (eq. 1), uncertainties computed using CATS software (*Williams, 2008*). Manual detection of offsets. Data analysis: M. Métois, LGLTPE.
- **S5** - Pyacs software (*Tran*, 2013; *Nocquet*, 2018). Least-square inversion of parametric model (eq. 1), uncertainties computed with white-noise approximation. Automatic detection and repair of discontinuities (outliers and offsets) with F-ratio test for the significance (99% confidence level minimum for robust detection) and reprocessing after manual verification of offsets. Data analysis: J.-L. Menut, J.-M. Nocquet, L. Rolland, M. Vergnolle, Geoazur. [2]
- **S6** - HECTOR software (*Bos et al., 2013*) and GeodeZYX Toolbox (*Sakic et al., 2019*). Maximum Likelihood estimation of velocities, annual and semi-annual parameters using white-and power-law noise. Offsets based on logsheet information + visual detection with a manual "point and click". Data analysis: P. Sakic, GFZ.
- **S7** - SARI software (*Santamaría-Gómez, 2019.*). Least-square inversion of parametric model (eq. 1), uncertainties computed using white-noise approximation. Manual detection of offsets. Data analysis: A. Santamaria, GET.
- **S8** - GeoTS software (*Gazeaux et al., in prep*). Joint estimation (least-square) of velocity, annual and semi-annual, and offsets with white and autoregressive noise. Offsets are detected using Hotelling statistics. Offset dates and noise characteristics are common to the 3 components. Data analysis: P. Valty, J. Gazeau, IGN.
- **S9** - TSView software (MIT, *http://www-gpsg.mit.edu/~tah/GGMatlab/#_tsview*). Least-square inversion of parametric model (eq. 1), uncertainties computed using colored-noise approximation. Manual detection of offsets. Data analysis: P. Vernant, GM.

[1] Solution S2 is used to compute velocity products by the EPOS GNSS processing center located at ISTerre. https://www.epos-ip.org/tcs/gnss-data-and-products/news/epos-gnss-data-and-products-presents-data-analysis-double-difference

[2] Except for the last step (reprocessing after manual visualization), Solution S5 is used by the RENAG Data Center to produce operational position time series for the RENAG-RESIF stations. http://renag.resif.fr/ts/charts/stop/

In addition, the average of all nine solutions is computed with equal weighting of all solutions:

- **S10** - unweighted average.

Method summary

- S1: statistics on velocities over one-year spread;
- S2, S4, S7 and S9: least-square inversion of a parametric model with offsets based on logs files or managed manually;
- S3, S5 and S8: least-square inversion of a parametric model with automatic offset detection (plus manual verification);
- S6: Maximum Likelihood Estimation with offset detection (plus manual verification based on log files).

Velocity uncertainty summary

- S1: statistics on velocities;
- S2 and S4: CATS full colored-noise estimation;
- S3, S6 and S8: colored-noise approximation;
- S5 and S7: white-noise approximation;
- S9: colored-noise approximation with autoregressive model.

3) Results and comparison with target velocities

Hereafter, the difference between an estimated velocity and the true (synthetic) velocity is referred to as a **bias** (i.e., the deviation from the expected result). In order to provide statistics for the whole dataset, we compute three statistical estimators of the biases:

- **dV_{50}**: median (50^{th} percentile) of the distribution of absolute values of biases;
- **dV_{95}**: 95^{th} percentile of the distribution of absolute values of biases;
- **dV_{RMS}**: Root-mean-square (RMS) of the distribution of biases.

Because of the limited number of synthetic data (105 series from 35 stations, 5 quality groups, 3 series durations), our study only provides first order results on the variability of velocity estimations from different methods and software. This small sample does not allow detailed analyses of specific parameter effects and such conclusions should not be drawn from our results.

A synthesis of each individual solution is provided in a summary figure (Figs. S1–S10 in Appendix 2) showing the estimated velocities versus the true velocities for the three components, as well as the distribution of the velocity biases relative to the associated velocity uncertainties.

Overall results organized per solutions (S1–S10) and per quality groups are shown in Figures 1 and 2. In all figures, a color code is used to represent the five quality groups and station codes: Super Clean / SC = dark green; Rather Clean / RC = light green; Mid Range / MR = light blue; Rather Ugly / RU = orange; Super Ugly / SU = red.

Individual solution statistics are given in Table 2 (excluding stations from group SU). In order to discuss the average quality of each solution, we use a simple metric that consist in counting the number of times a given solution falls in the best three (upper tier) or worst three (lower tier) for each component (N, E, U) and statistical indicator (dV_{50}, dV_{95}, dV_{RMS}). Each solution overall score consists in the ratio N upper tier / N lower tier; e.g., a score of 2 / 4 indicates that the solution appears twice in the upper tier and four times in the lower tier (over a total of nine indicators).

Result 1. To first order, all nine solutions are associated with horizontal (resp. vertical) velocity biases smaller than 1.0 mm/a (resp. 2.0 mm/a) of the same magnitudes.

Result 2. No single solution stands out as significantly better or worse than the others (Figs. 1 and 2). However, our simple classification of the solutions in the upper and lower tiers indicates three main categories (Table 2):

- Solutions S3, S4 and S10 (unweighted average) are significantly more often in the upper tier than in the lower tier; Solution S7 also falls in this category but with slightly lower score;
- Solutions S1, S2, S5 and S8 are more often in the lower tier than in the upper tier;
- Solutions S6 and S9 are as often in the upper and lower tiers.

Result 3. Velocity biases for stations from groups SC–RU, representative of standard GNSS data, vary between ca. 0.1 and 2.0 mm/a depending on the component (N, E, U) and indicator (Table 2). Specifically:

- **Median biases (dV_{50}) are ca. 0.1 mm/a (horizontal components) and 0.1–0.3 mm/a (vertical component).**
  - dV_{50} = 0.04–0.11 mm/a North comp.;
  - dV_{50} = 0.04–0.15 mm/a East comp.;
  - dV_{50} = 0.07–0.36 mm/a Up comp.

- **The 95th percentiles (dV_{95}) show a large variability between solutions, ca. 0.2–0.7 mm/a (horizontal components) and 0.5–2.0 mm/a (vertical component).**
  - dV_{95} = 0.23–0.53 mm/a North comp.;
  - dV_{95} = 0.24–0.71 mm/a East comp.;
  - dV_{95} = 0.43–2.03 mm/a Up comp.

- **RMS of biases (dV_{RMS}) are positioned between the median and 95th statistics, ca. 0.1–0.3 mm/a (horizontal components) and 0.3–0.9 mm/a (vertical component).**
  - dV_{RMS} = 0.14–0.24 mm/a North comp.;
  - dV_{RMS} = 0.13–0.28 mm/a East comp.;
  - dV_{RMS} = 0.28–0.96 mm/a Up comp.

The differences between the North and East components in all indicators reflect the higher noise amplitude (daily dispersion) of the latter (cf. Table 1).

Table 2. Velocity bias statistics for the nine solutions (S1–S9) and average (S10). *Statistics are given in mm/a for the 28 stations in quality groups SC, RC, MR and RU (SU stations are not included, cf. Section 1). Solutions flagged in green / red are in upper / lower tier for a given component and indicator (line). The last line (Score) gives the total result for a given solution as number of upper tier (green) / lower tier (red) classifications.*

		S1	S2	S3	S4	S5	S6	S7	S8	S9	*S10*
	dV_{50}	0.09	0.11	0.04	0.05	0.07	0.05	0.07	0.08	0.06	*0.05*
North	**dV_{95}**	0.26	0.53	0.26	0.23	0.41	0.33	0.31	0.26	0.27	*0.23*
	dV_{RMS}	0.16	0.24	0.14	0.18	0.23	0.16	0.15	0.16	0.13	*0.13*
	dV_{50}	0.15	0.07	0.05	0.06	0.06	0.04	0.06	0.12	0.11	*0.06*
East	**dV_{95}**	0.38	0.71	0.35	0.24	0.51	0.42	0.35	0.65	0.52	*0.32*
	dV_{RMS}	0.21	0.28	0.22	0.13	0.23	0.19	0.16	0.28	0.23	*0.14*
	dV_{50}	0.36	0.16	0.10	0.13	0.21	0.11	0.17	0.14	0.07	*0.13*
Up	**dV_{95}**	2.03	1.54	0.43	0.83	0.98	1.81	0.77	1.07	1.01	*1.04*
	dV_{RMS}	0.96	0.74	0.28	0.44	0.46	0.71	0.46	0.47	0.77	*0.42*
Score		**1 / 5**	**0 / 7**	**8 / 0**	**7 / 1**	**1 / 4**	**3 / 2**	**5 / 1**	**1 / 4**	**4 / 4**	***7 / 0***

Result 4. The vertical (Up) component is associated with velocity biases ca. 2–5 times larger than the horizontal components and with a stronger variability between solutions (Table 2, Figs. 1 and 2). This effect is likely due to the larger noise amplitude coupled with larger offset amplitudes compared to the horizontal components. As a result, the various offset management methods yield a higher variability in the velocity estimations.

In particular, **solution S1 (MIDAS method)** stands out as slightly worse than the others on the three indicators for the vertical component (Table 2). This might point out a need for better tuning of the method for series with high noise / large offsets. In contrast, **solution S3 (automatic offset detection)** provides better results than the others for the dV_{95} and dV_{RMS} of the vertical component, suggesting that automatic offset detection may be a better alternative in these cases (compared to manual detection).

Result 5. The unweighted average of all nine solutions (S10) yields results systematically in the upper tier of all individual solutions (Table 2, Figs. 1 and 2).

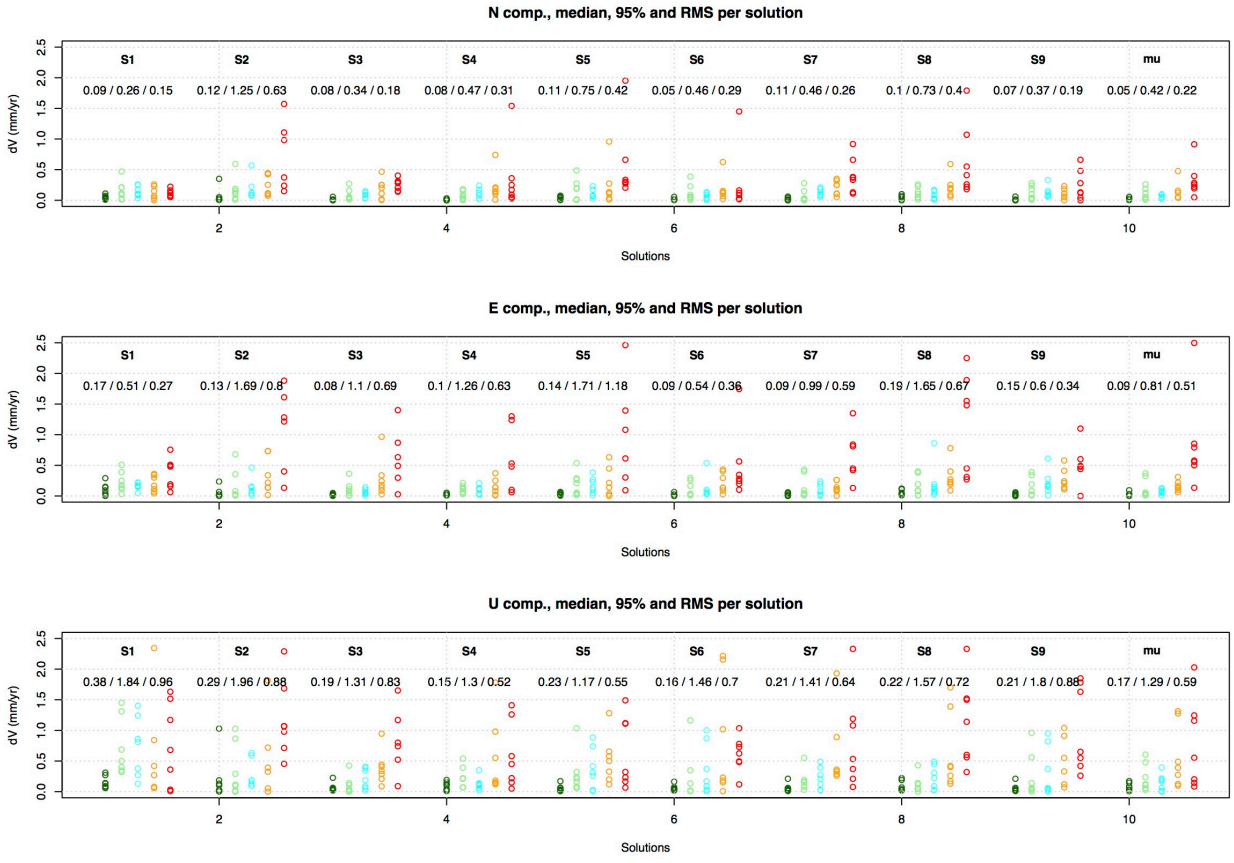

Figure 1. Velocity biases organized first per solutions and then per quality groups. *Absolute value of the velocity bias of each station is represented by a circle for individual solutions and for the average. Results in each solution are grouped by quality indicated by colors*

(from SC to SU = green to red, cf. text). For each solution the median, 95th percentile and RMS of all stations are given in mm/yr (NB: these statistics include stations from group SU, in contrast with those in Table 2). N, E, U : North, East and Vertical components.

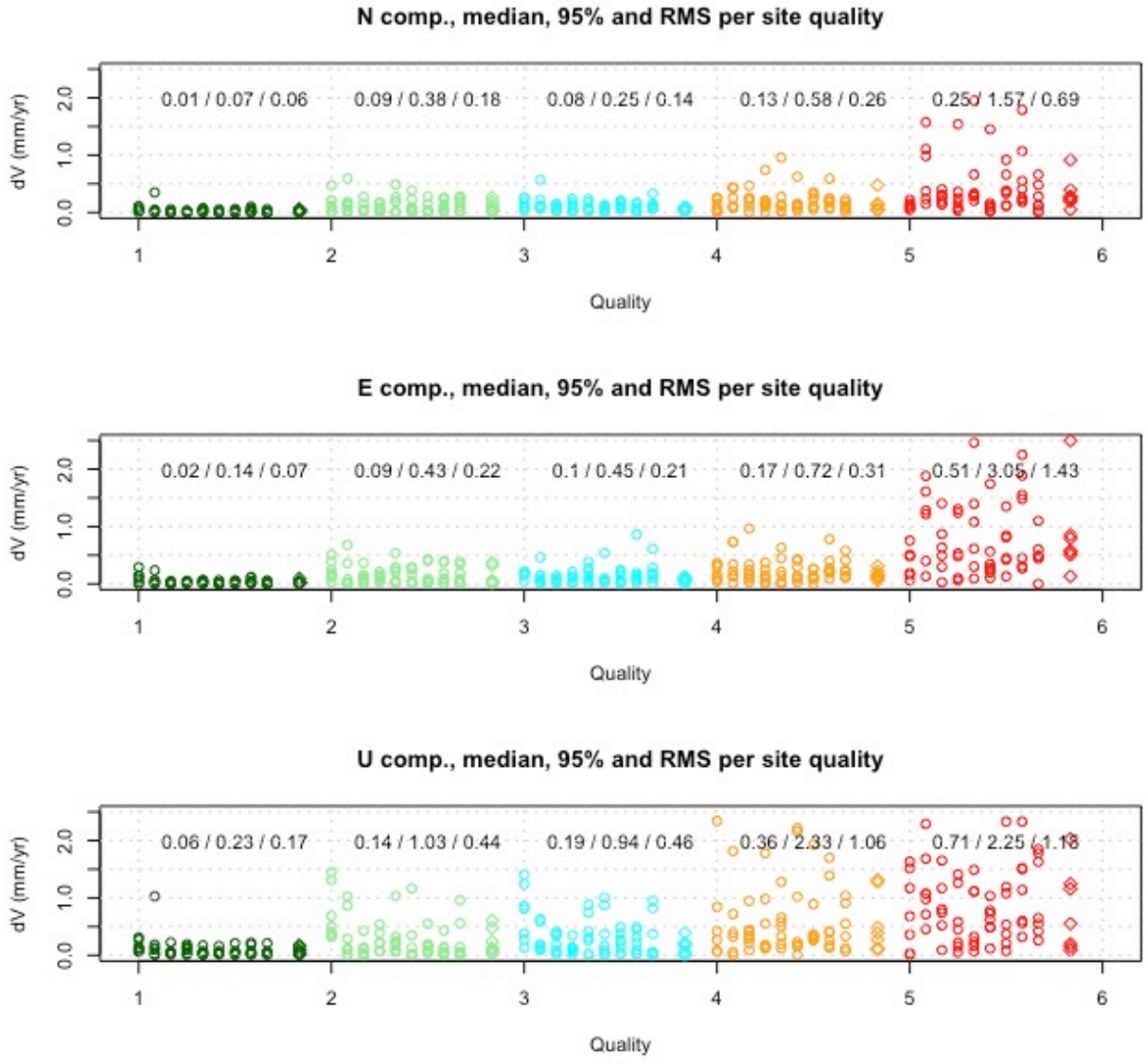

Figure 2. Velocity biases organized first per quality groups and then per solutions. *Absolute value of the velocity bias of each station is represented by a circle for individual solutions (1.0 = S1, 1.1 = S2 … 1.8 = S9; 2.0 = S1, 2.1 = S2 …) and a diamond for the average. Solutions are grouped by quality indicated by colors (from SC to SU = green to red, cf. text). For each quality group the median, 95th percentile and RMS of all solutions (S1–S9) are given in mm/a. N, E, U : North, East and Vertical components.*

Result 6. To first order, the effect of the time series duration can be estimated by comparing the series of 10–12, 19 and 29 years. This effect is shown in Figure 3 (excluding series from quality group SU). As expected, the lengthening of the series duration yields a decrease of the velocity biases. This decrease is non-linear and strongly sensitive to the series parameters:

- **Lengthening of series from 10–12 to 19 years results in a decrease of velocity biases ca. 50%,** varying between 30% and 80% depending on the qualities and components.
- **Lengthening of series from 19 to 29 years results in a decrease of velocity biases ca. 25%,** varying between 6% and 60% depending on the qualities and components (with one case of increase by 15%, probably an example of bad statistics from the small sample).

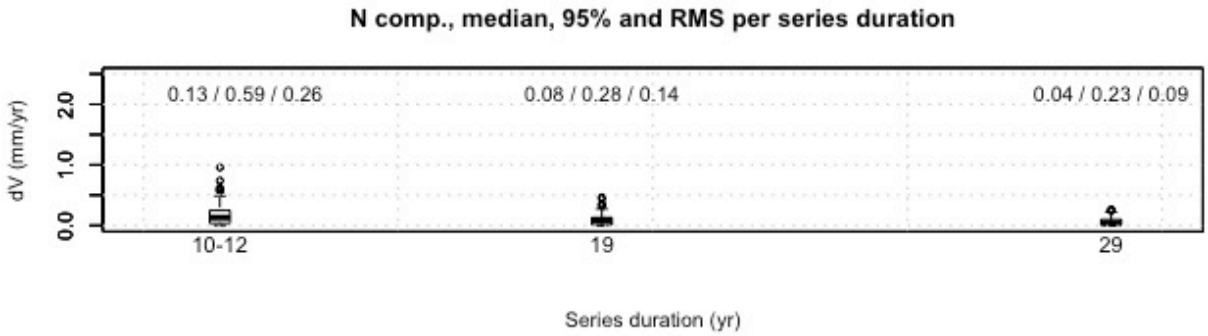

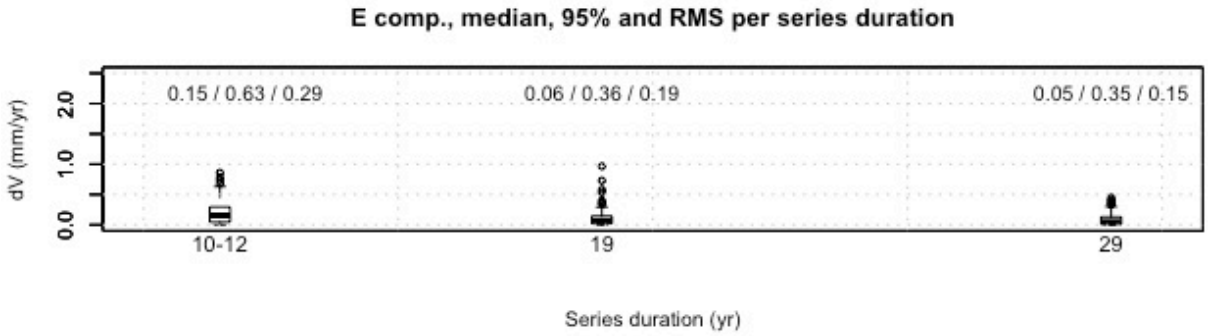

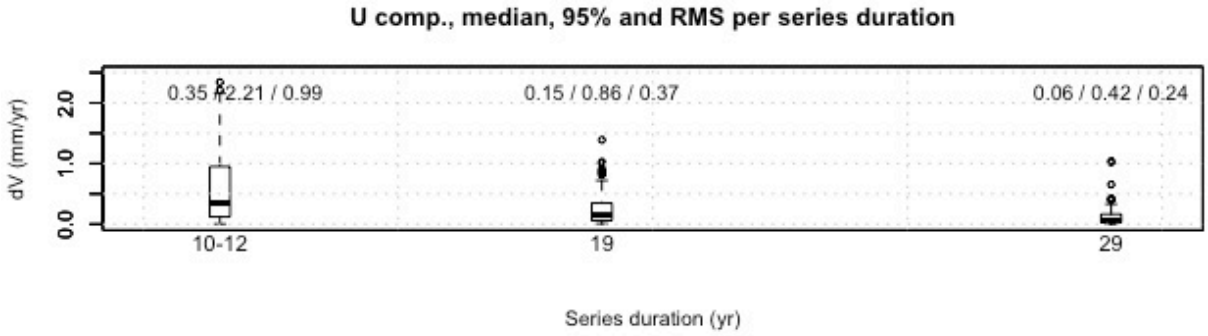

Figure 3. Velocity biases organized per series durations. *Absolute values of the velocity biases (excluding quality group SU) are shown as box plots (quartiles and outliers). The median, 95th percentile and RMS are given for each duration (10–12, 19 and 29 years).*

Result 7. The nine solutions are associated with different methods to estimate the velocity formal uncertainties (standard errors, cf. Section 2). Assuming a Gaussian distribution of the velocity estimations, these uncertainties should be such that 68.3% (resp. 95.4%) of the velocity biases are inferior to 1 (resp. 2) times the standard errors. The comparison of the velocity biases relative to their standard errors for each solution (Appendix 2) allows the following observations:

- **Methods based on colored-noise models (solutions S2, S3, S4, S6 and S8) yield reasonable estimations of the velocity standard errors** (although on average slightly too small): 80–91% of the velocity biases are inferior to twice their standard errors.
- Unsurprisingly, **methods based on white-noise models (solutions S5 and S7) yield standard errors systematically too small**: only 20–25% of the velocity biases are inferior to twice their standard errors. Average dV / σ ratios vary between 6 and 14, suggesting standard errors too small by a factor of 3–7.
- The **MIDAS method (solution S1) yields standard errors systematically too large**, especially for the horizontal components for which 100% of the velocity are smaller than twice their standard errors. dV / σ ratios suggest that the standard errors are too large by a factor ca. 2.
- The **TSView "Real Sigma" method (solution S9) yields standard errors slightly too small**, with ca. 60% of the velocity biases inferior to twice their standard errors (average dV / σ ratios ca. 2).

Bibliography

Benoist, C. (2018). Prise en compte de la dépendance spatiotemporale des séries temporelles de coordonnées GNSS pour une meilleure détermination des plaques tectoniques majeures par rapport au centre de la Terre. *Thèse de Doctorat de l'Observatoire de Paris*.

Blewitt, G., C. Kreemer, W.C. Hammond, and J. Gazeaux (2016). MIDAS robust trend estimator for accurate GPS station velocities without step detection*, Journal of Geophysical Research*, 121, doi:10.1002/2015JB012552.

Bos, M. S., Fernandes, R. M. S., Williams, S. D. P., & Bastos, L. (2013). Fast error analysis of continuous GNSS observations with missing data. *Journal of Geodesy*, 87(4), 351–360. doi:10.1007/s00190-012-0605-0.

Gazeaux, J., Williams, S. D. P., King, M. A., Bos, M. S., Dach, R., Deo, M., Moore, A. W., Ostini, L., Petrie, E. J., Roggero, M., Teferle, N. F., Olivares, G. and Webb, F. H. (2013). Detecting offsets in GPS time series: First results from the detection of offsets in GPS experiment, *Journal of Geophysical Research*, 118(5), 2397–2407, doi:10.1002/jgrb.50152.

Kasdin, N.J. (1995). Discrete Simulation of Colored Noise and Stochastic Processes and 1/f^a Power Law Noise Generation, *Proceedings of the IEEE*, 83 (5), 802-827.

Masson, C., Mazzotti, S. and Vernant, P. (2019). Precision of continuous GPS velocities from statistical analysis of synthetic time series, *Solid Earth*, 10, 329–342, doi:10.5194/se-10-329-2019.

Nocquet, J.-M. (2018). Pyacs: A set of Python tools for GPS analysis and tectonic modelling. *Wegener Conference*, Strasbourg, France.

R Core Team (2016). R: A language and environment for statistical computing. R Foundation for Statistical Computing, Vienna, Austria. URL https://www.R-project.org/.

Sakic, P., Mansur, G., Chaiyaporn, K., and Ballu, V. (2019). The geodeZYX toolbox: a versatile Python 3 toolbox for geodetic-oriented purposes. V. 4.0. GFZ Data Services. http://doi.org/10.5880/GFZ.1.1.2019.002.

Santamaría-Gómez, A. (2019). SARI: interactive GNSS position time series analysis software. *GPS solutions*, 23:52. doi: 10.1007/s10291-019-0846-y.

Tran, D. T. (2013). Analyse rapide et robuste des solutions GPS pour la tectonique. *PhD thesis*, Université de Nice Sophia Antipolis.

Williams, S.D.P. (2008). CATS: GPS coordinate time series analysis software, *GPS Solut,* 12, 147-153. doi: 10.1007/s10291-007-0086-4.

Appendix 1. Synthetic time series

Each figure shows the daily position series of the station North, East and Up components (in mm) as a function of the date (in yr). The orange vertical bars indicate the dates of offsets imposed in the series. Cf. text for station codes.

Station SC01

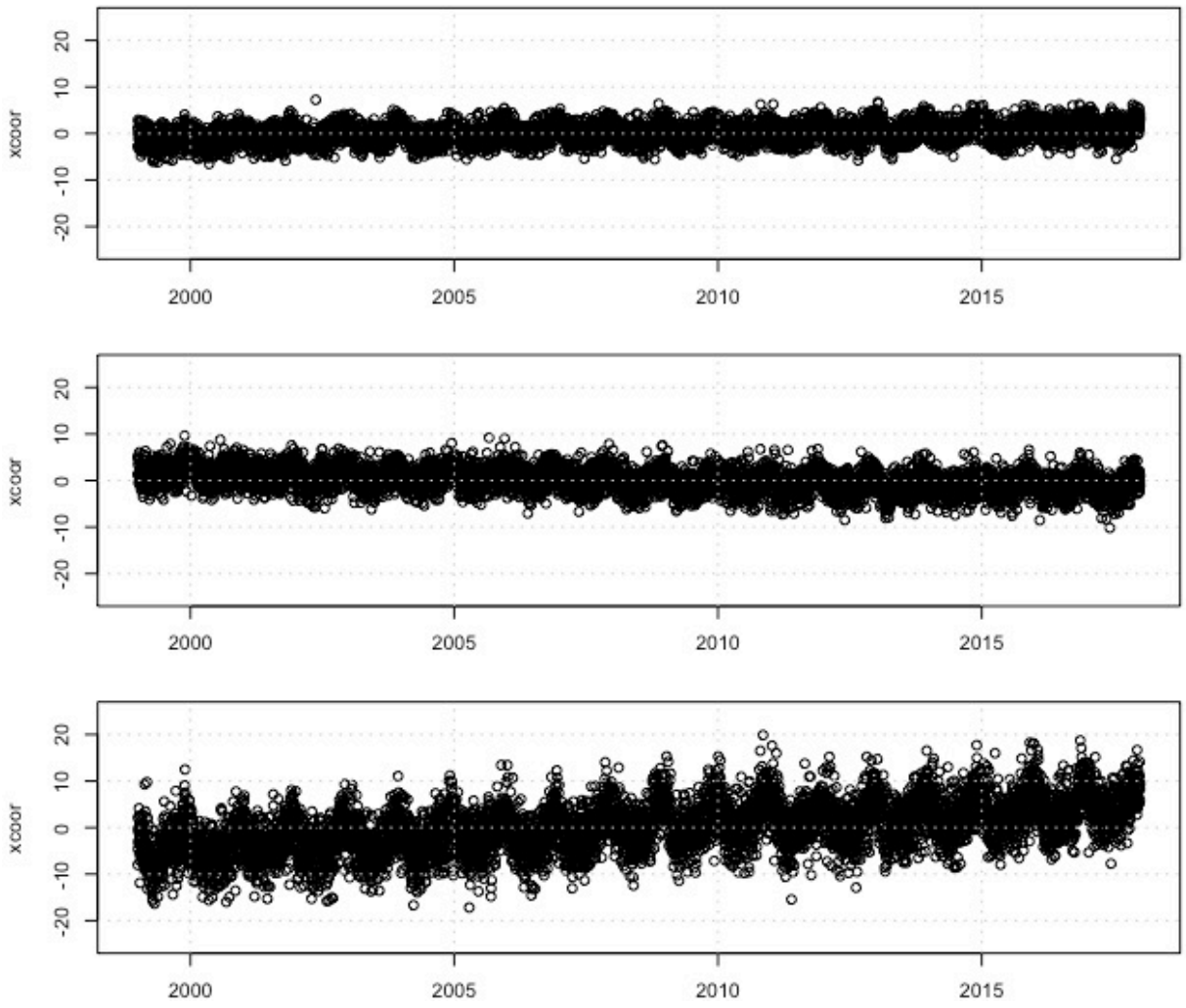

Station SC02

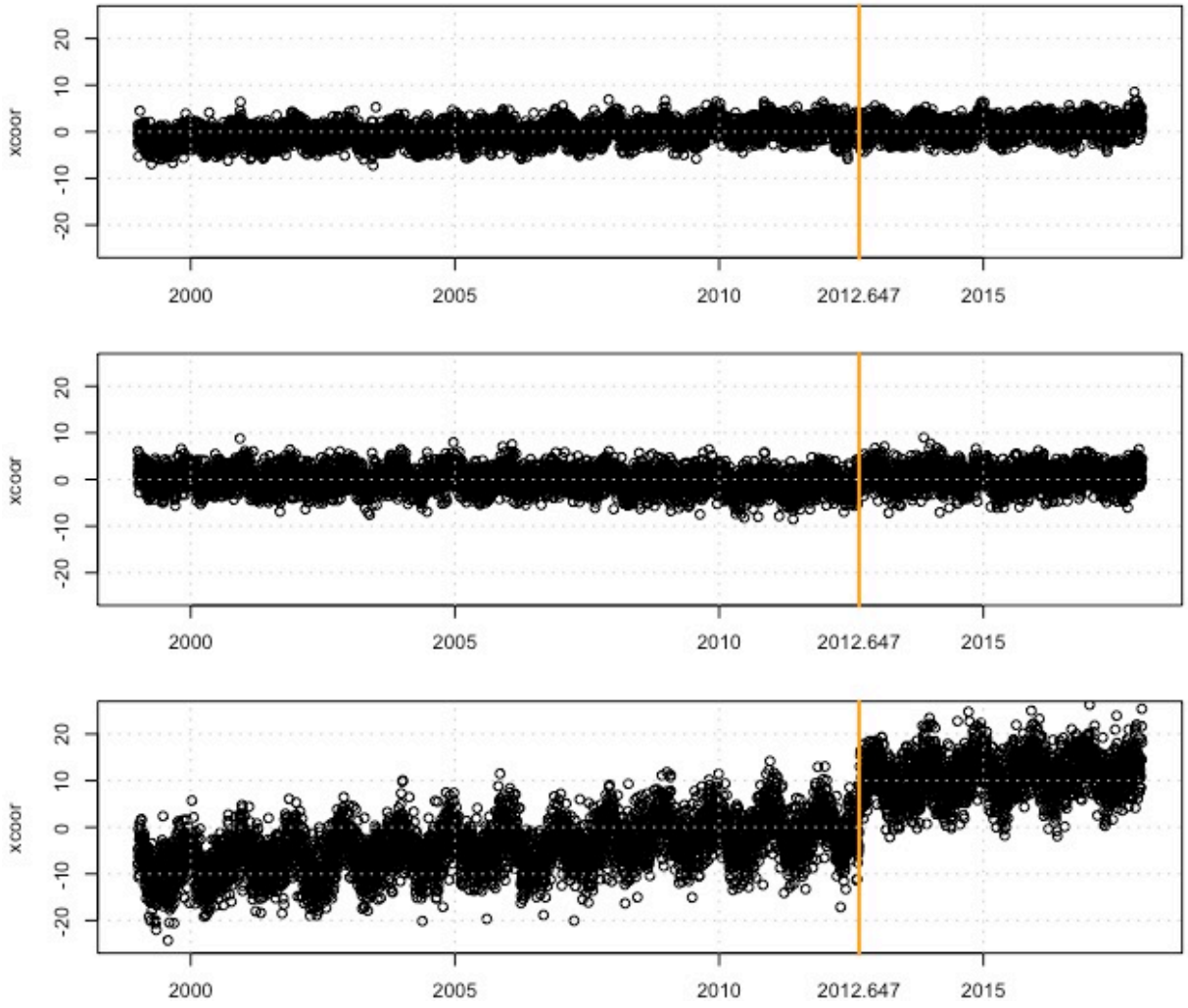

Station SC03

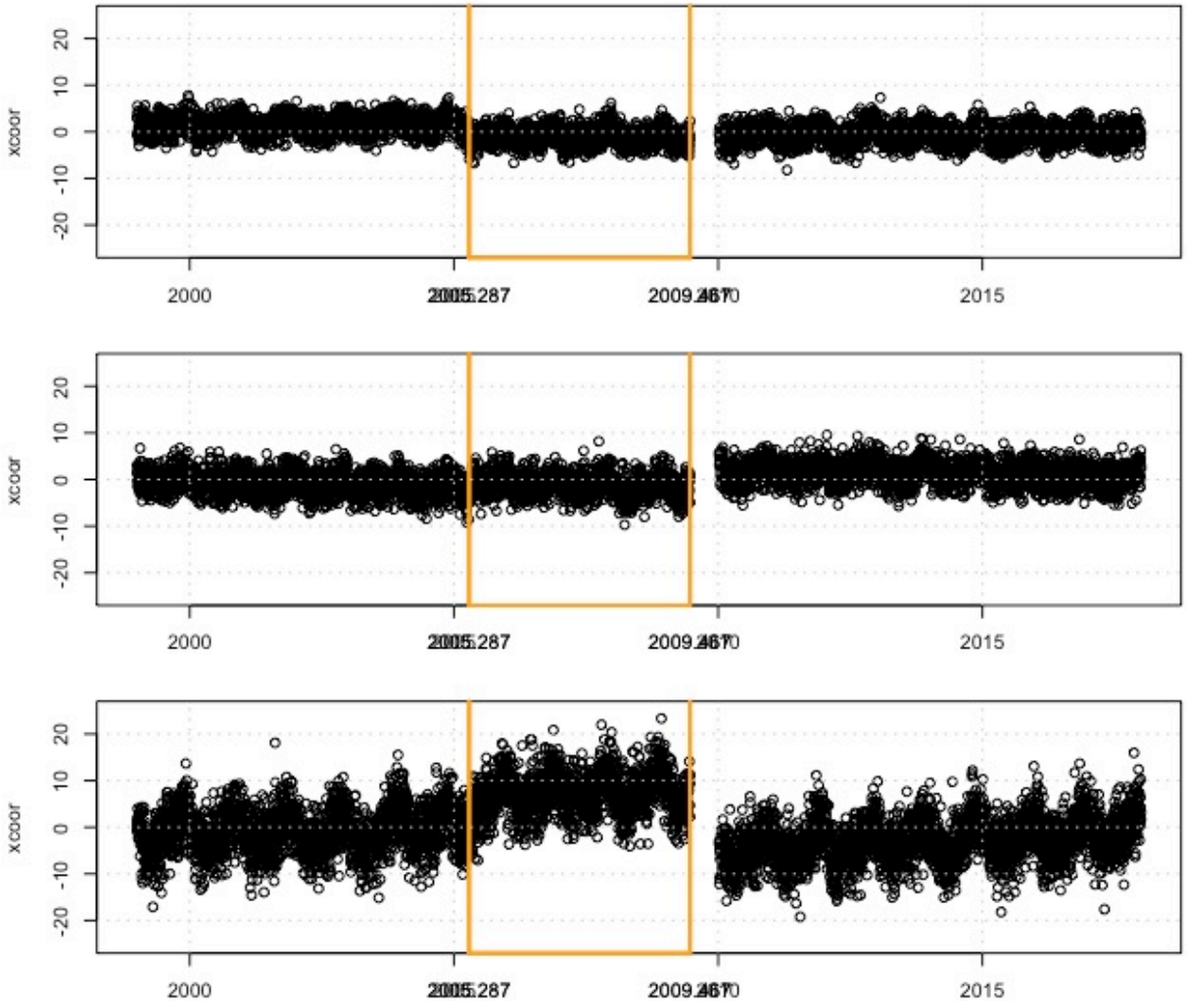

Station SC04

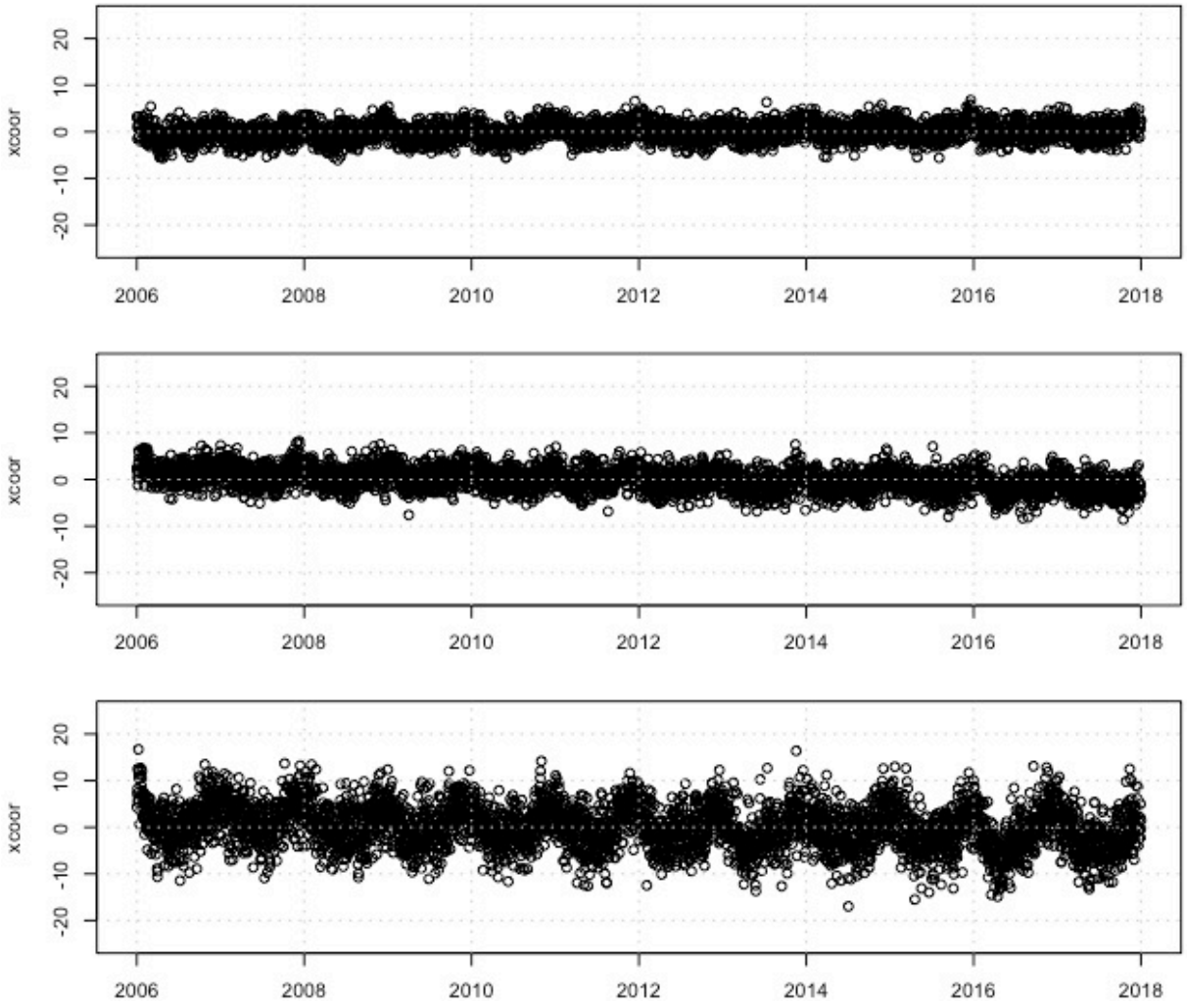

Station SC05

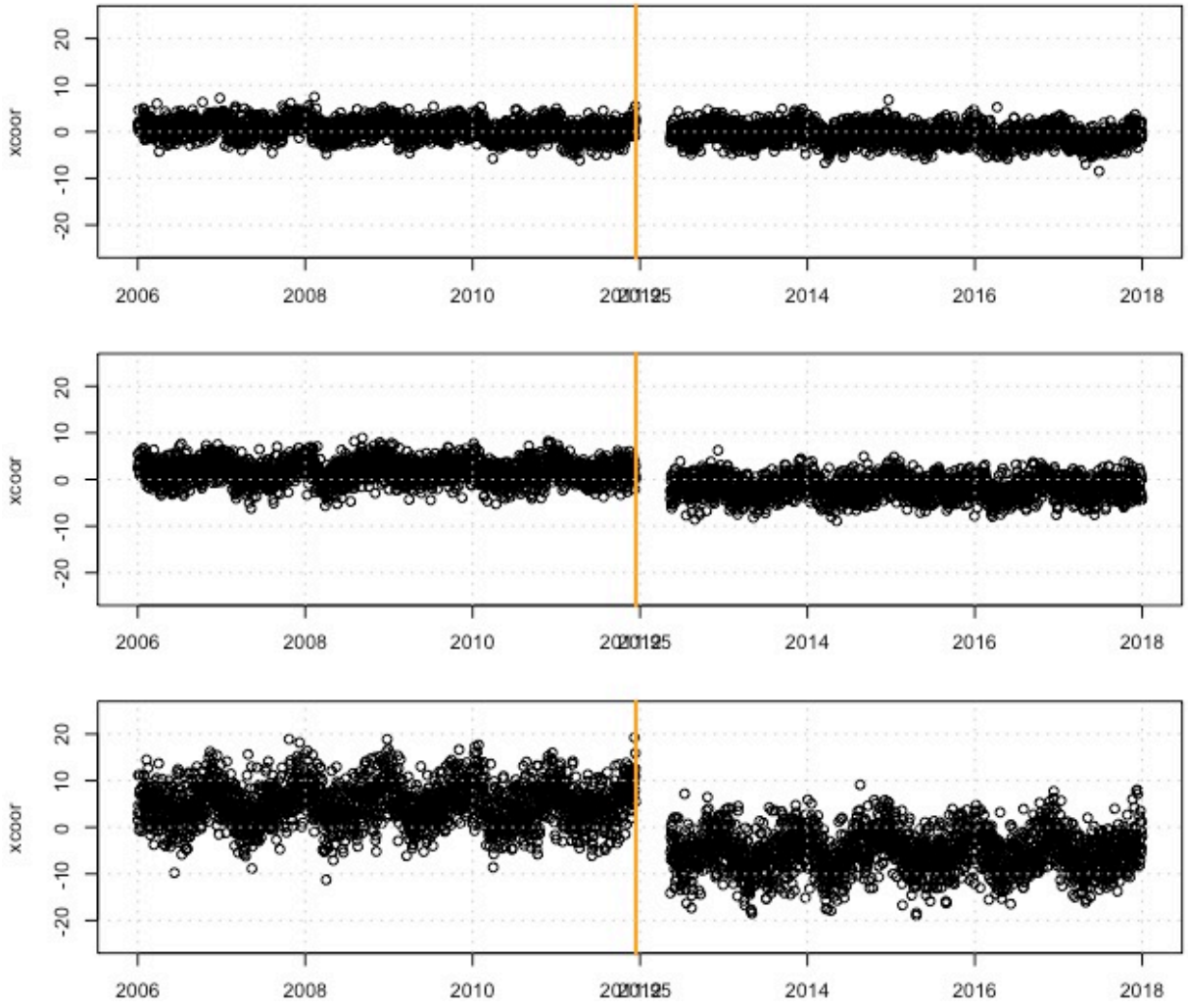

Station SC06

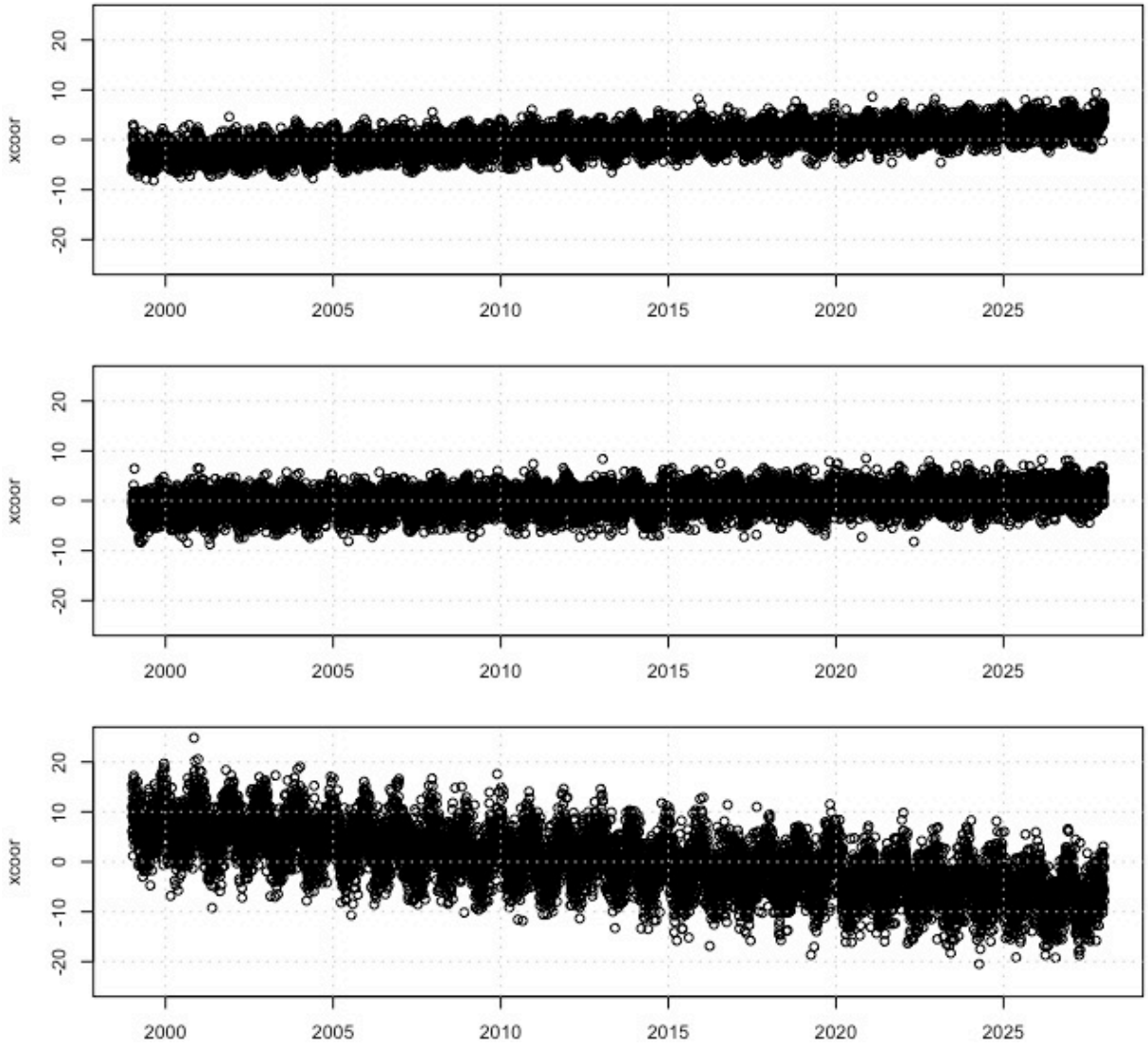

Station SC07

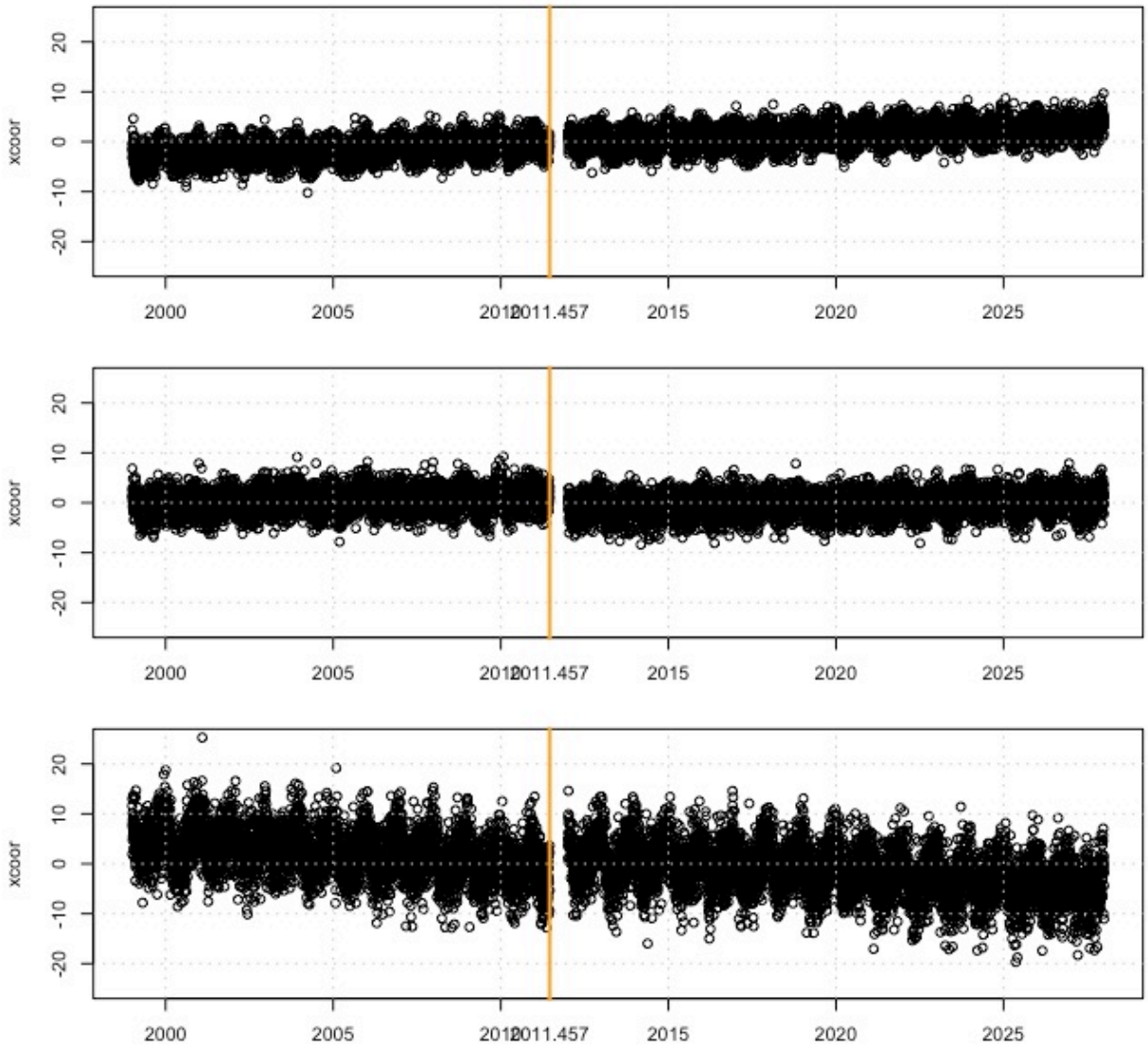

Station RC01

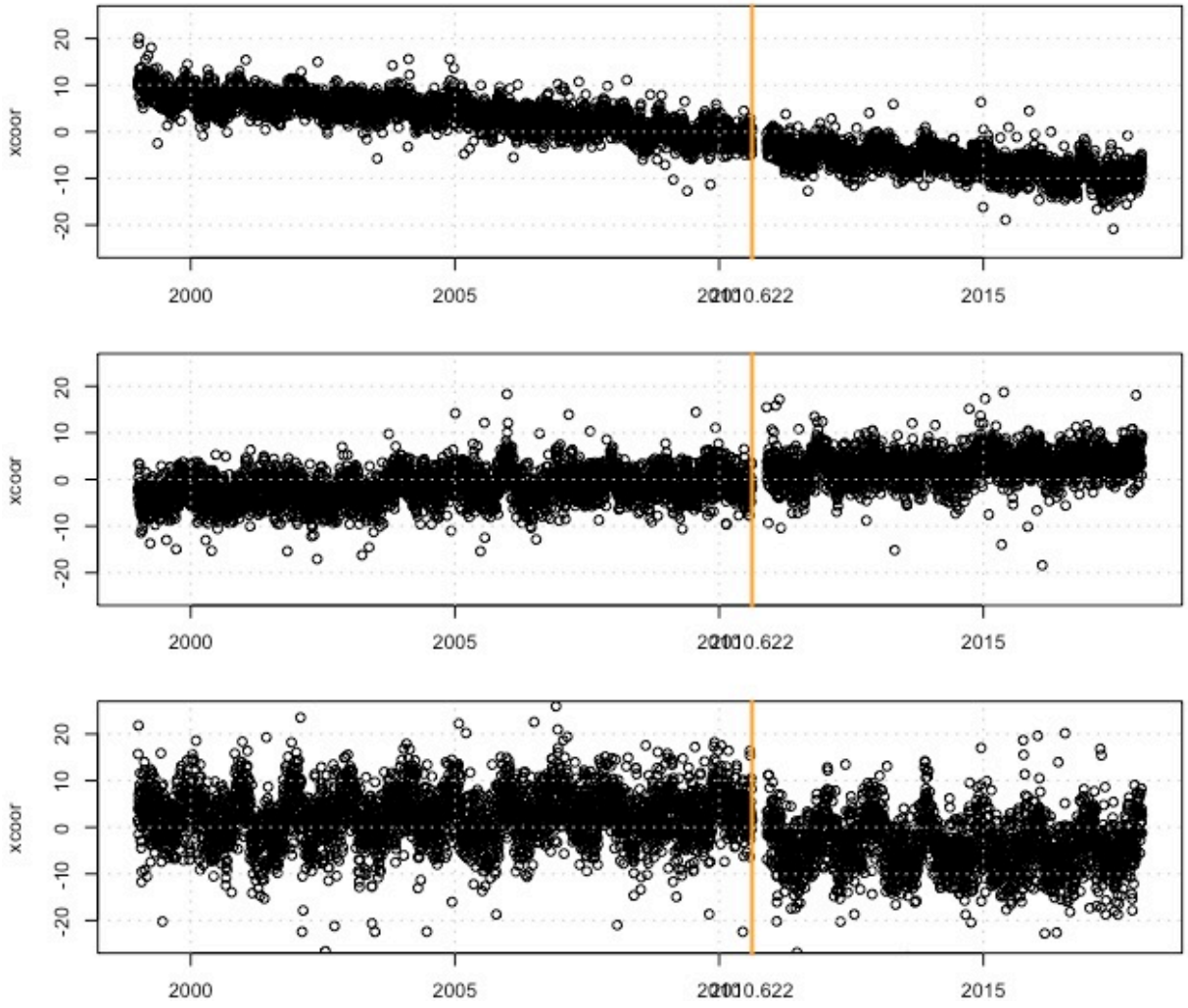

Station RC02

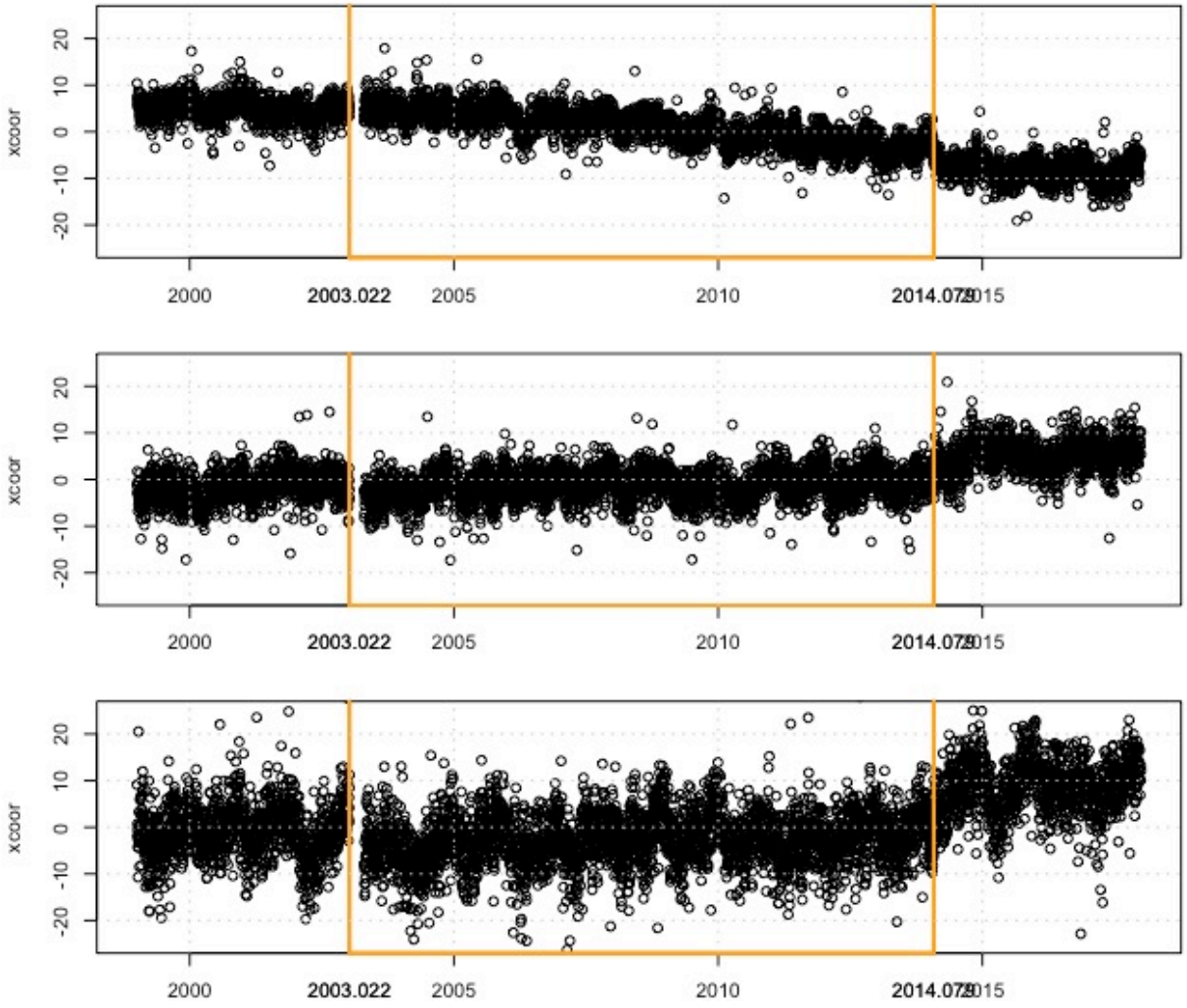

Station RC03

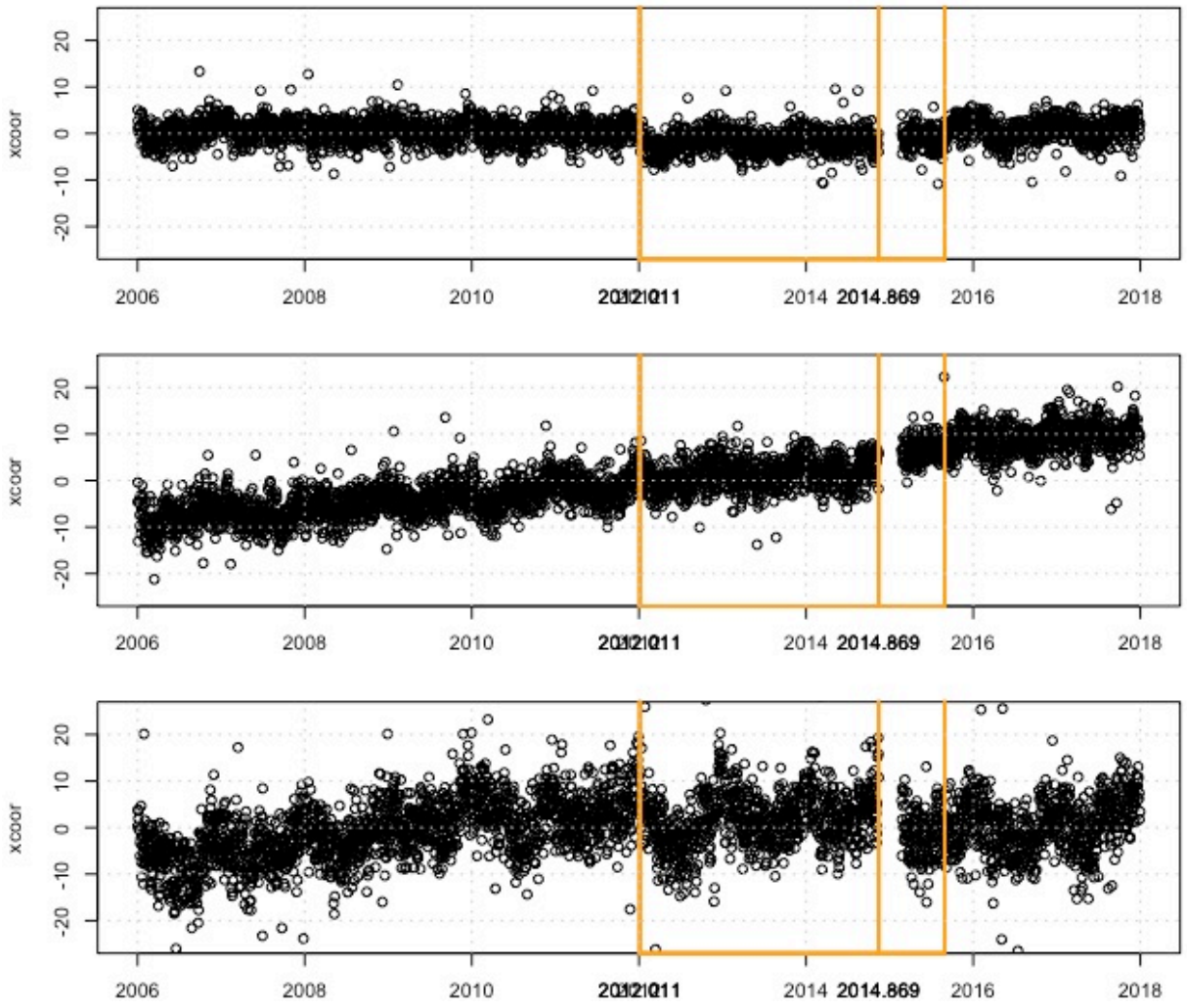

Station RC04

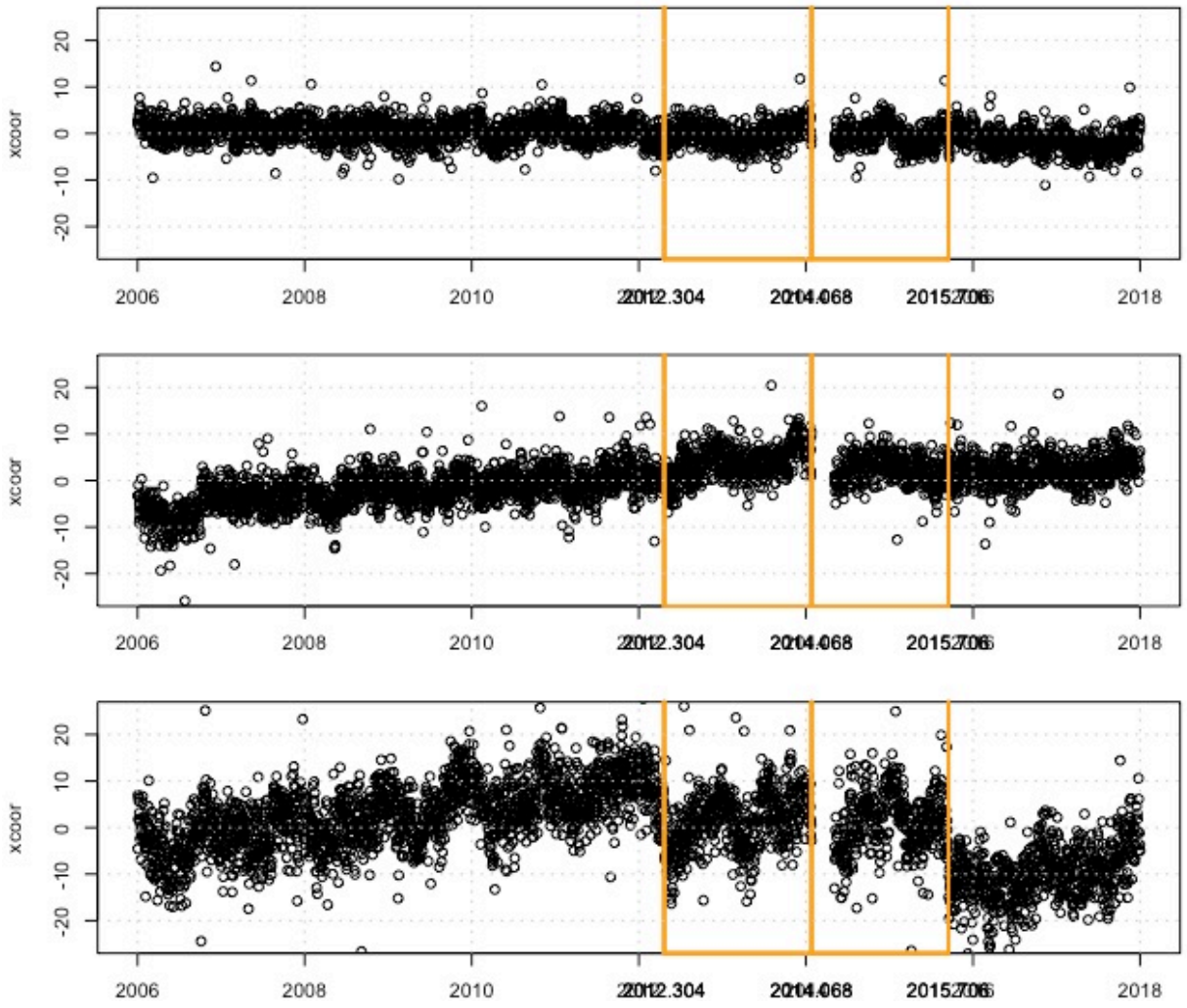

Station RC05

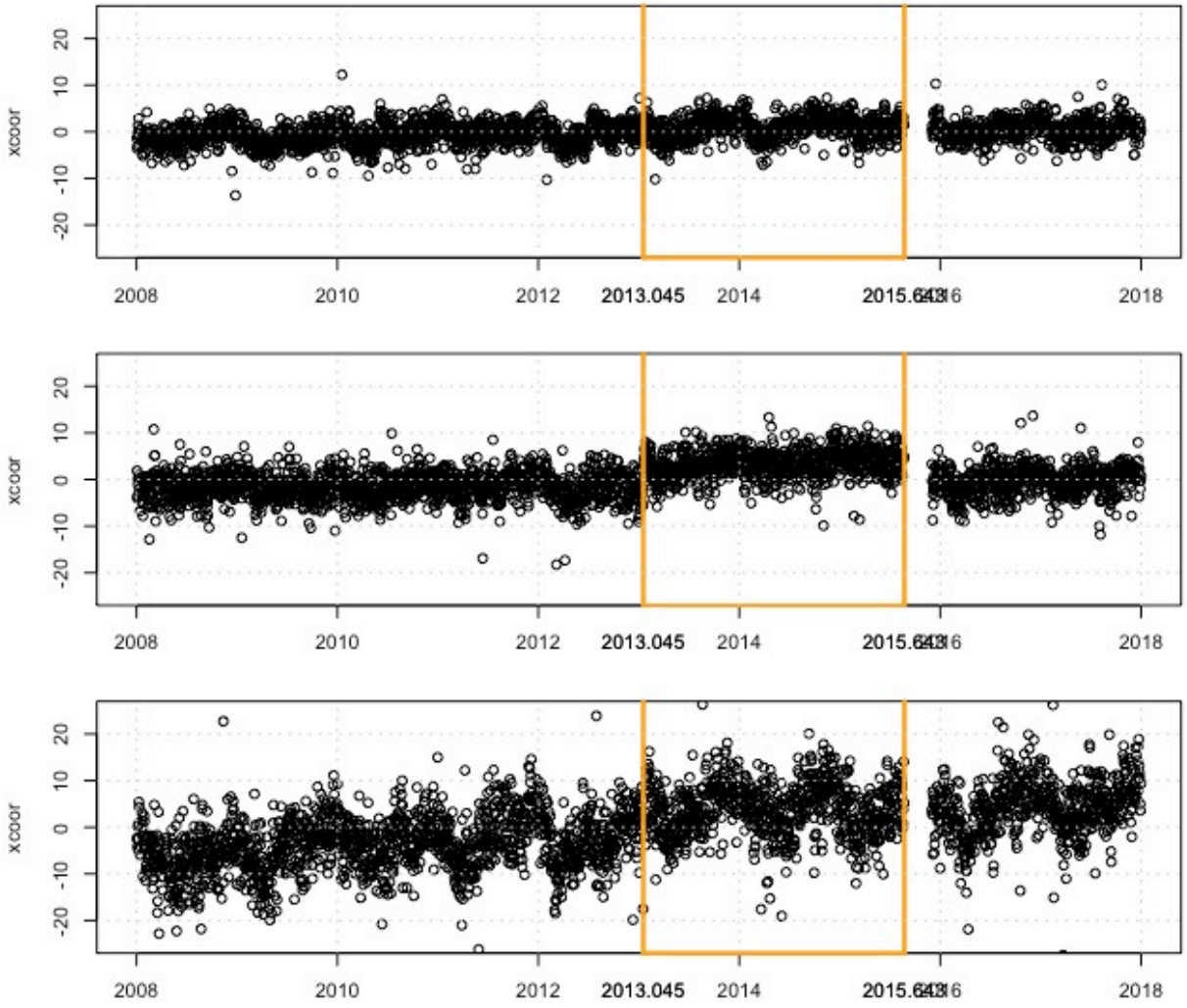

Station RC06

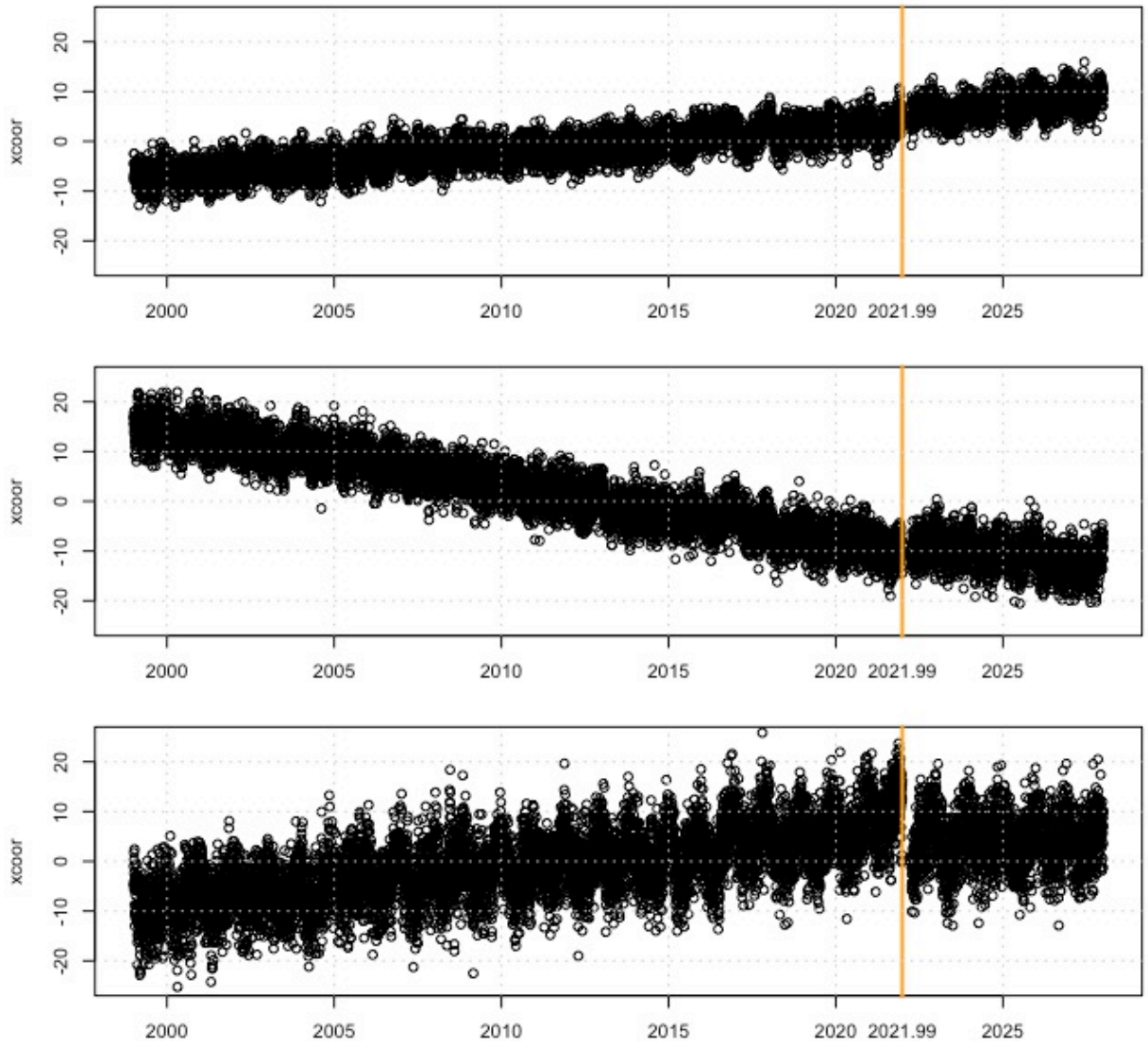

Station RC07

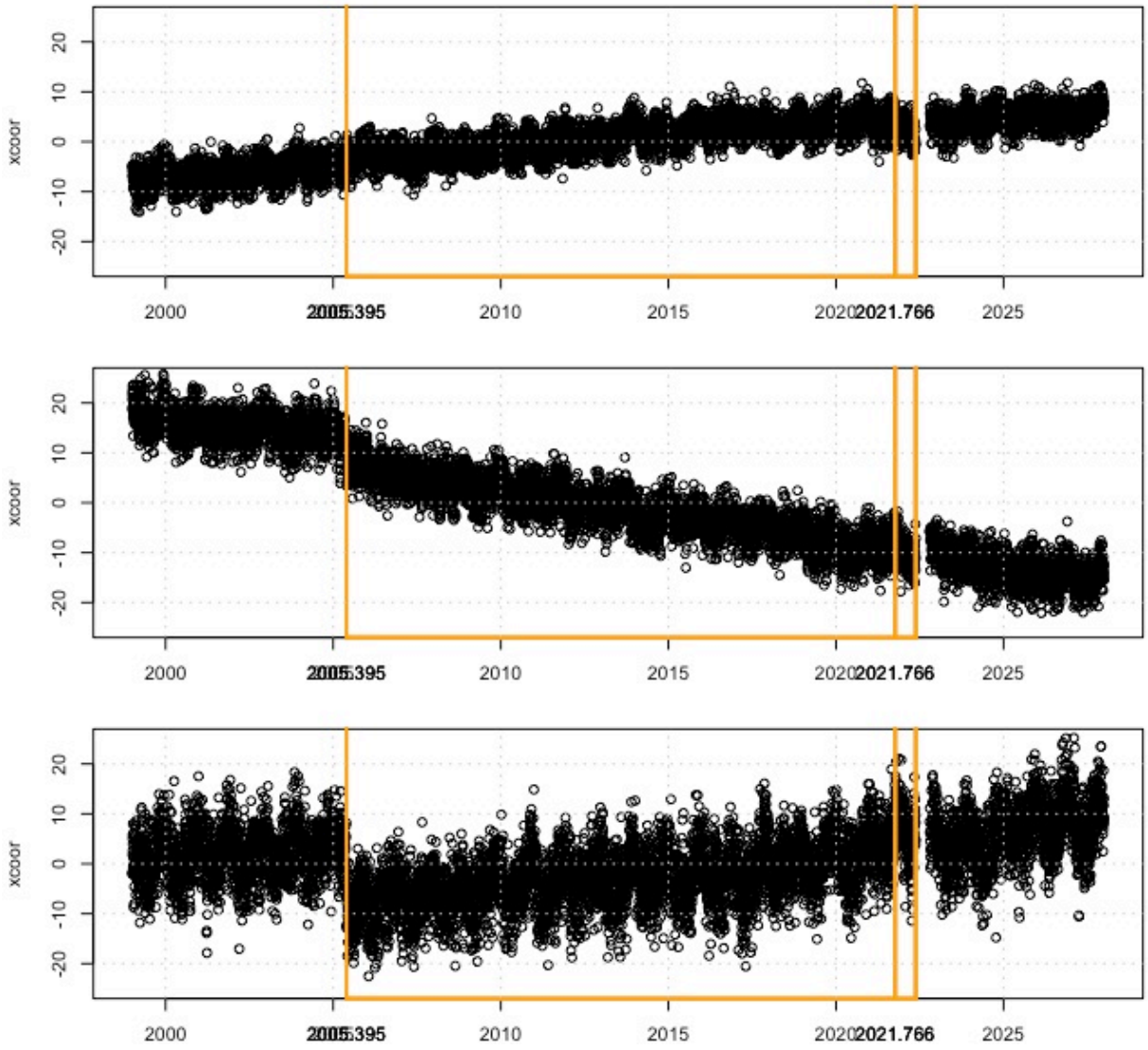

Station MR01

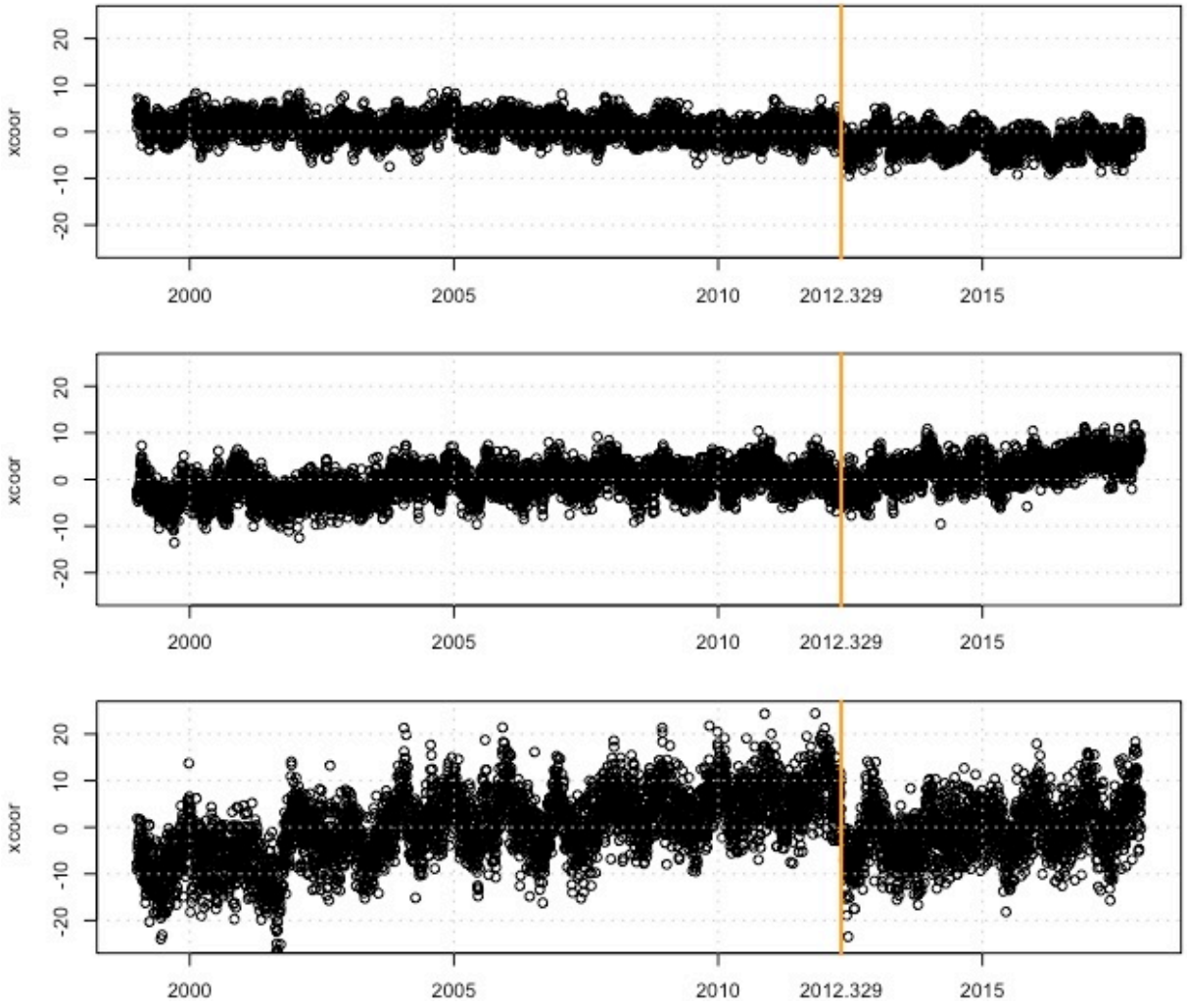

Station MR02

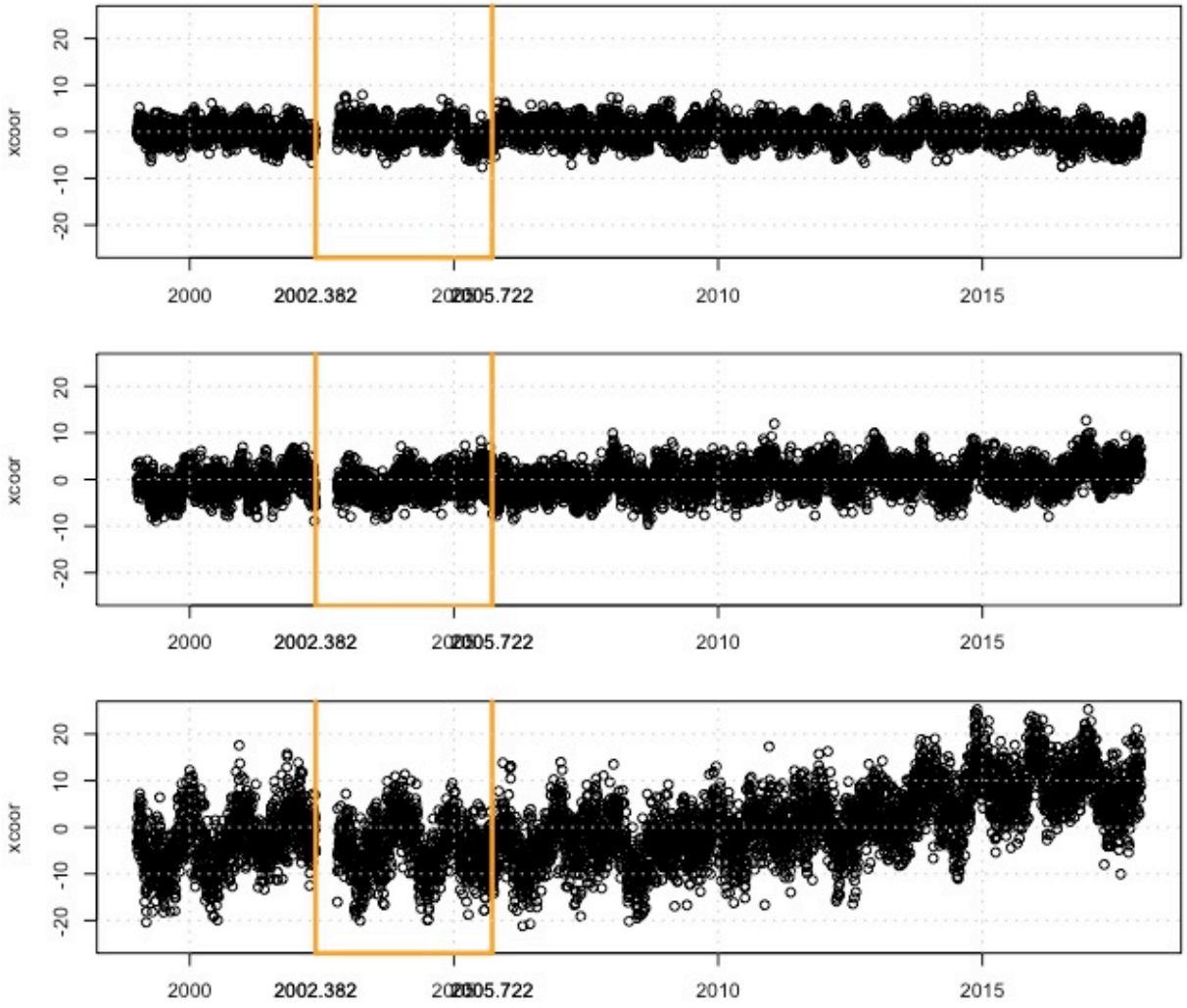

Station MR03

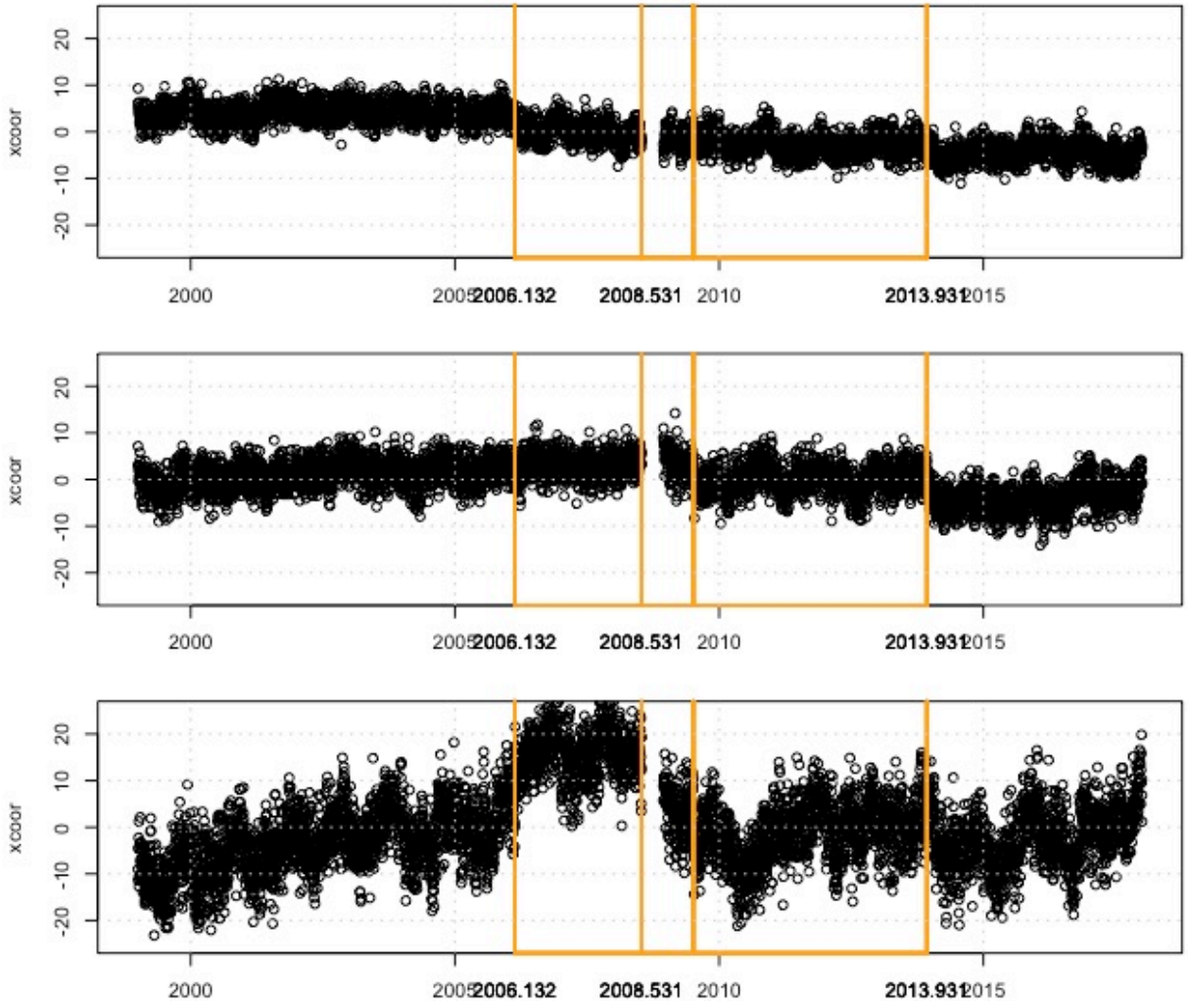

Station MR04

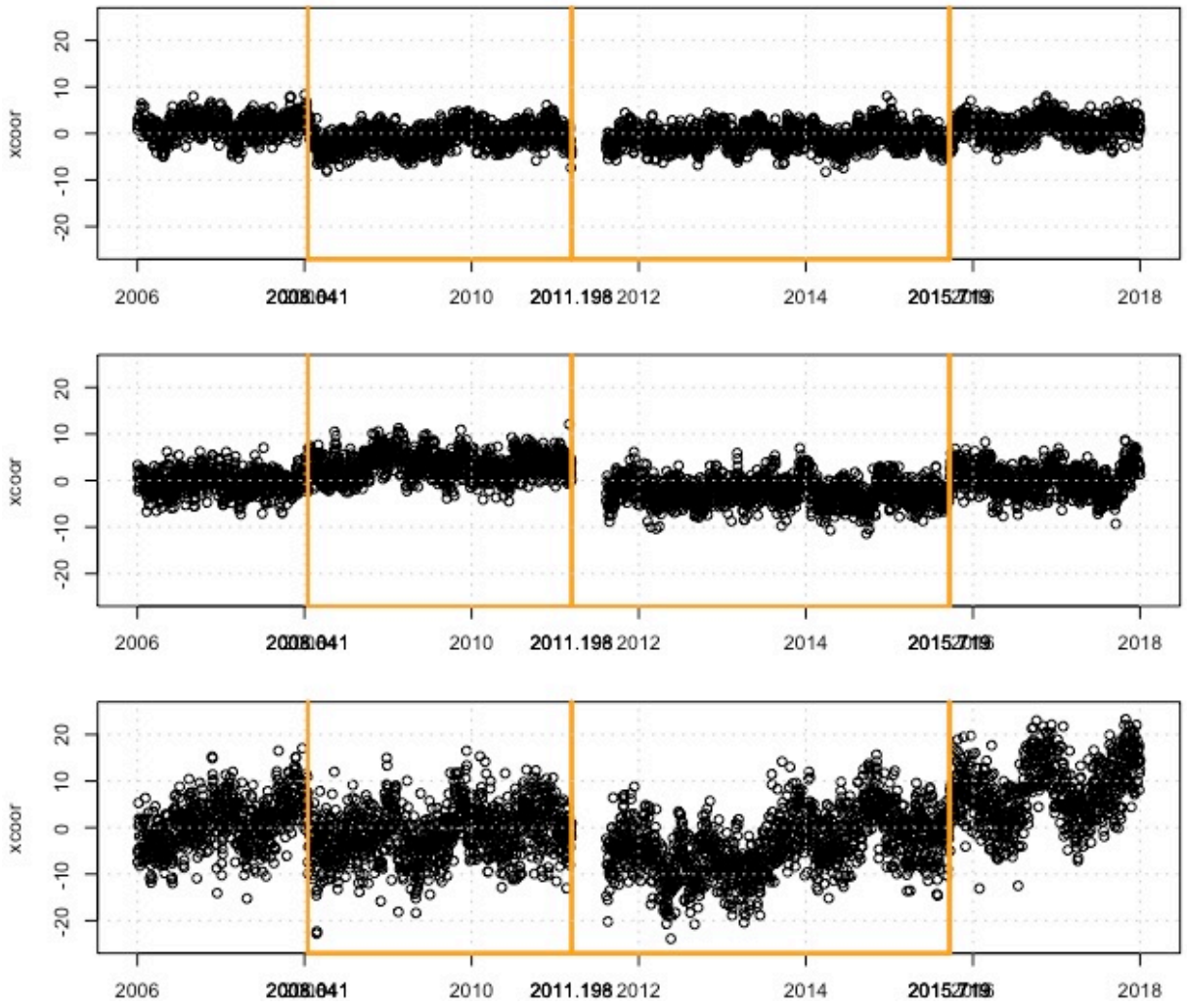

Station MR05

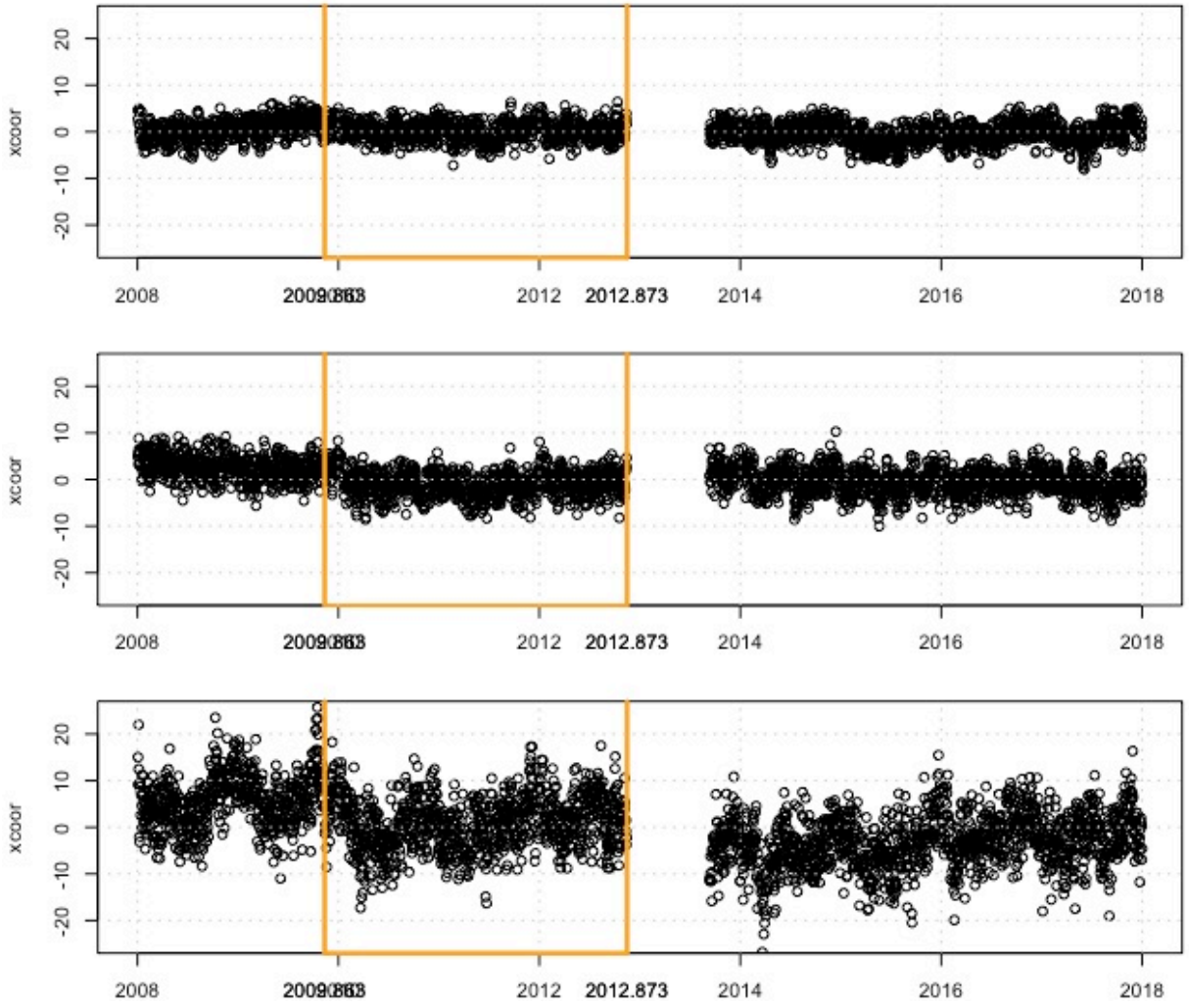

Station MR06

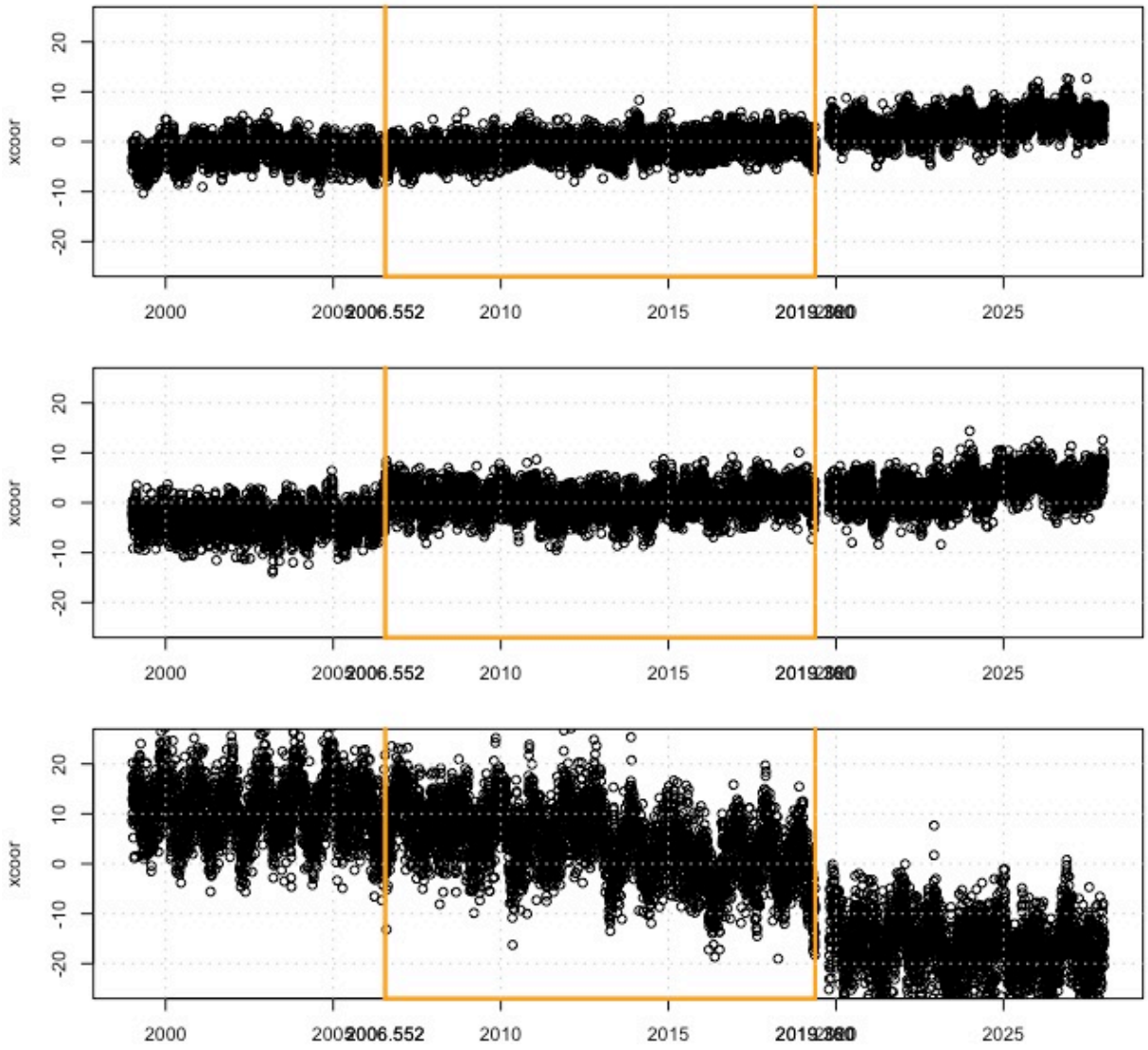

Station MR07

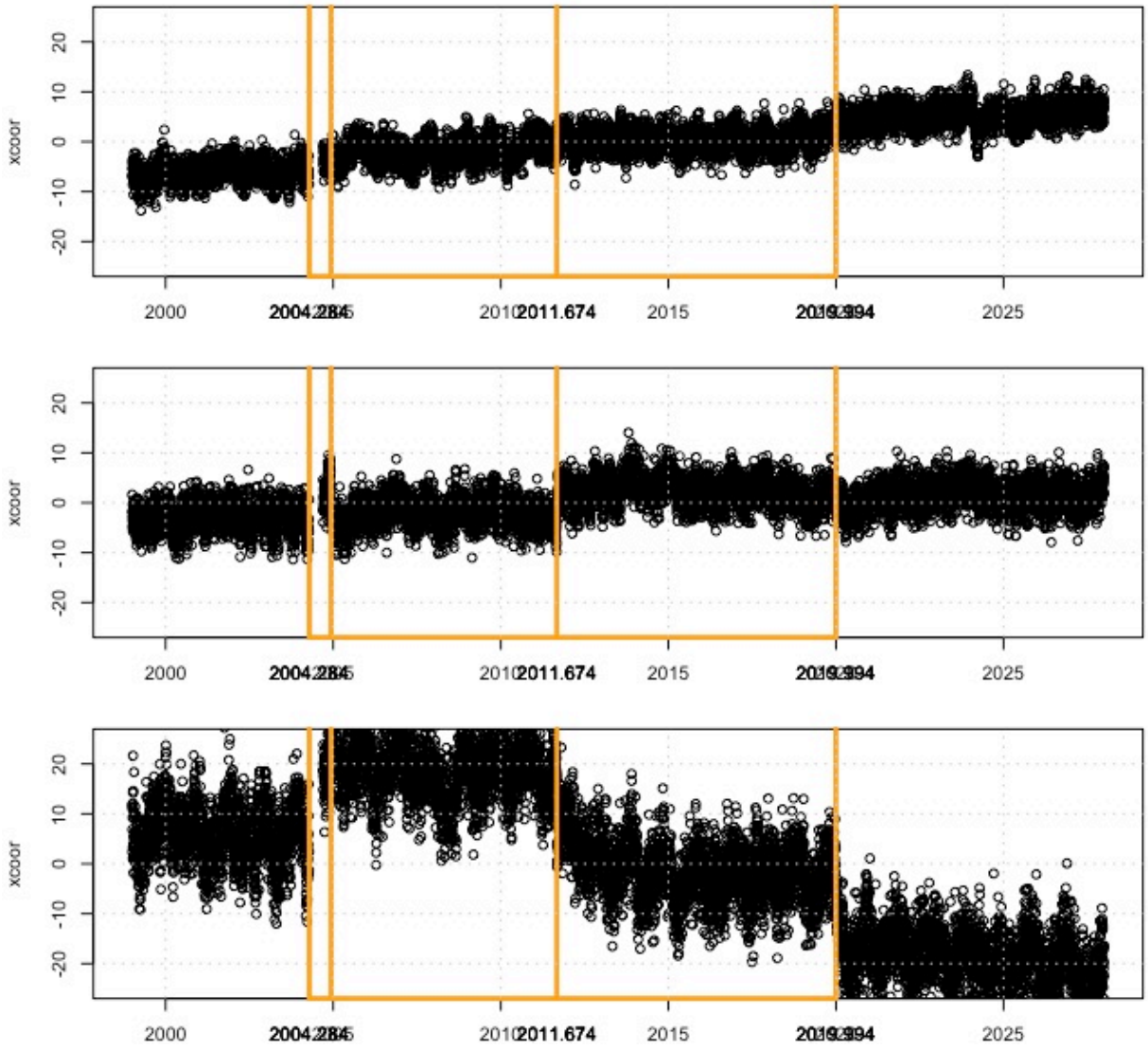

Station RU01

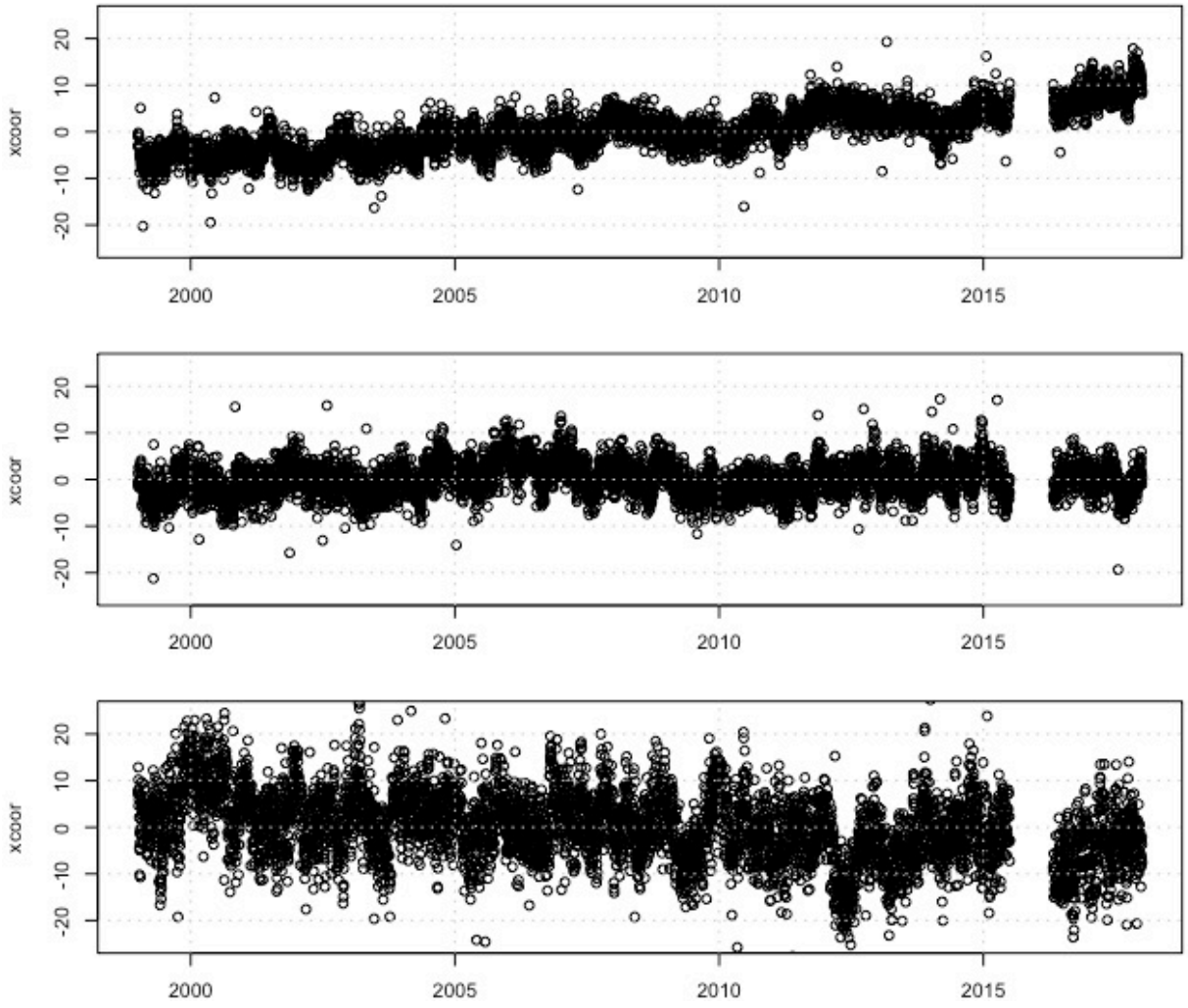

Station RU02

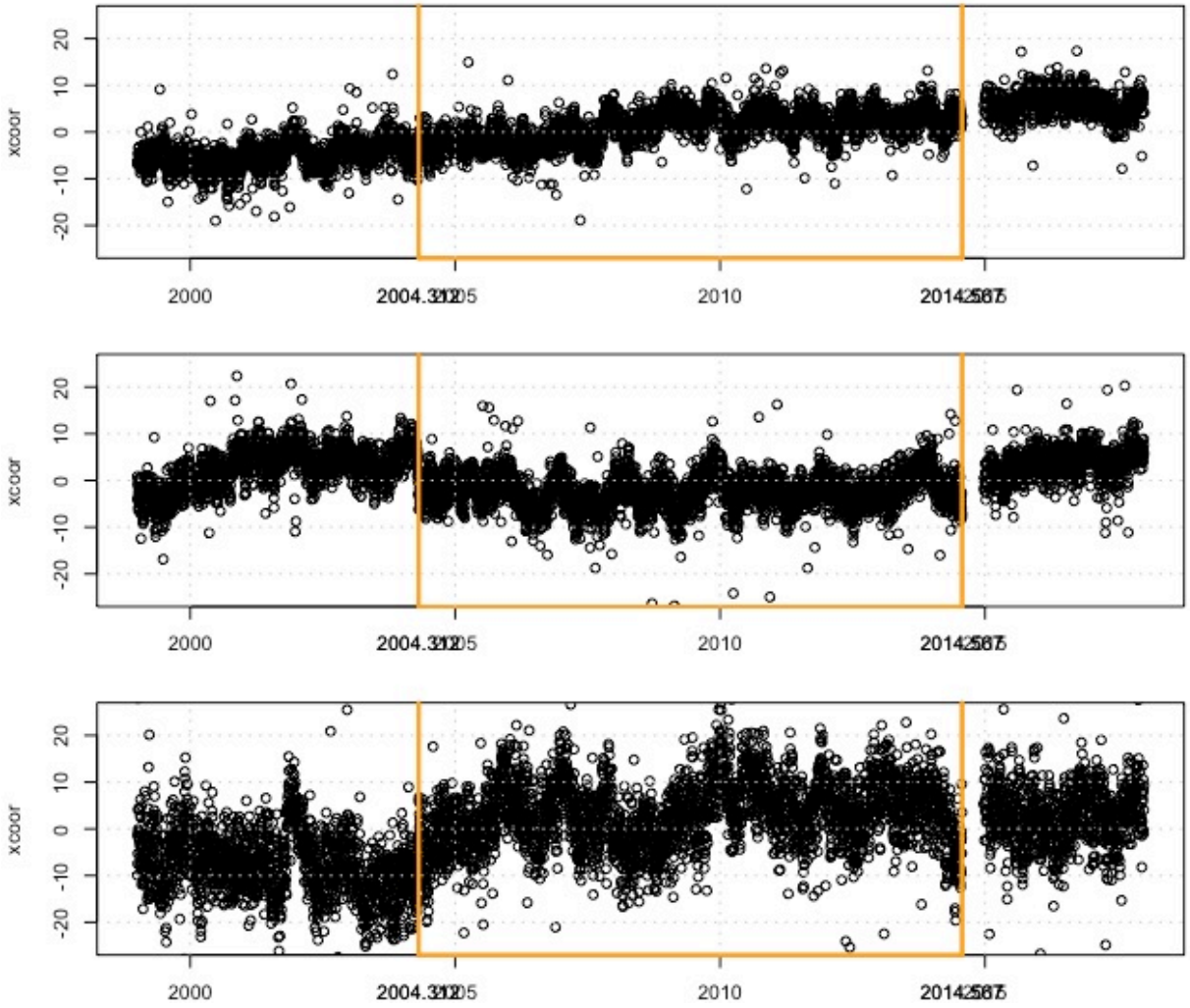

Station RU03

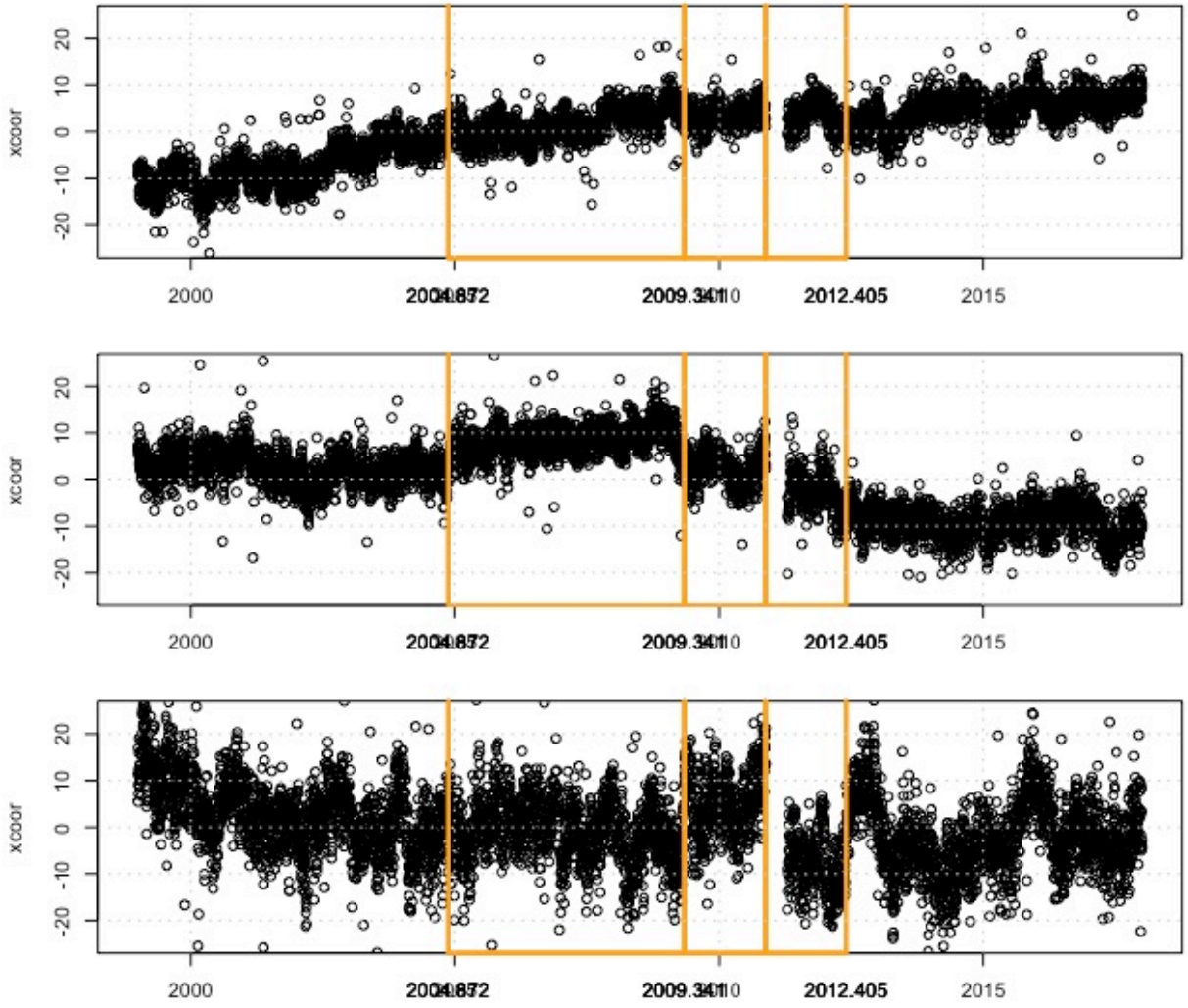

Station RU04

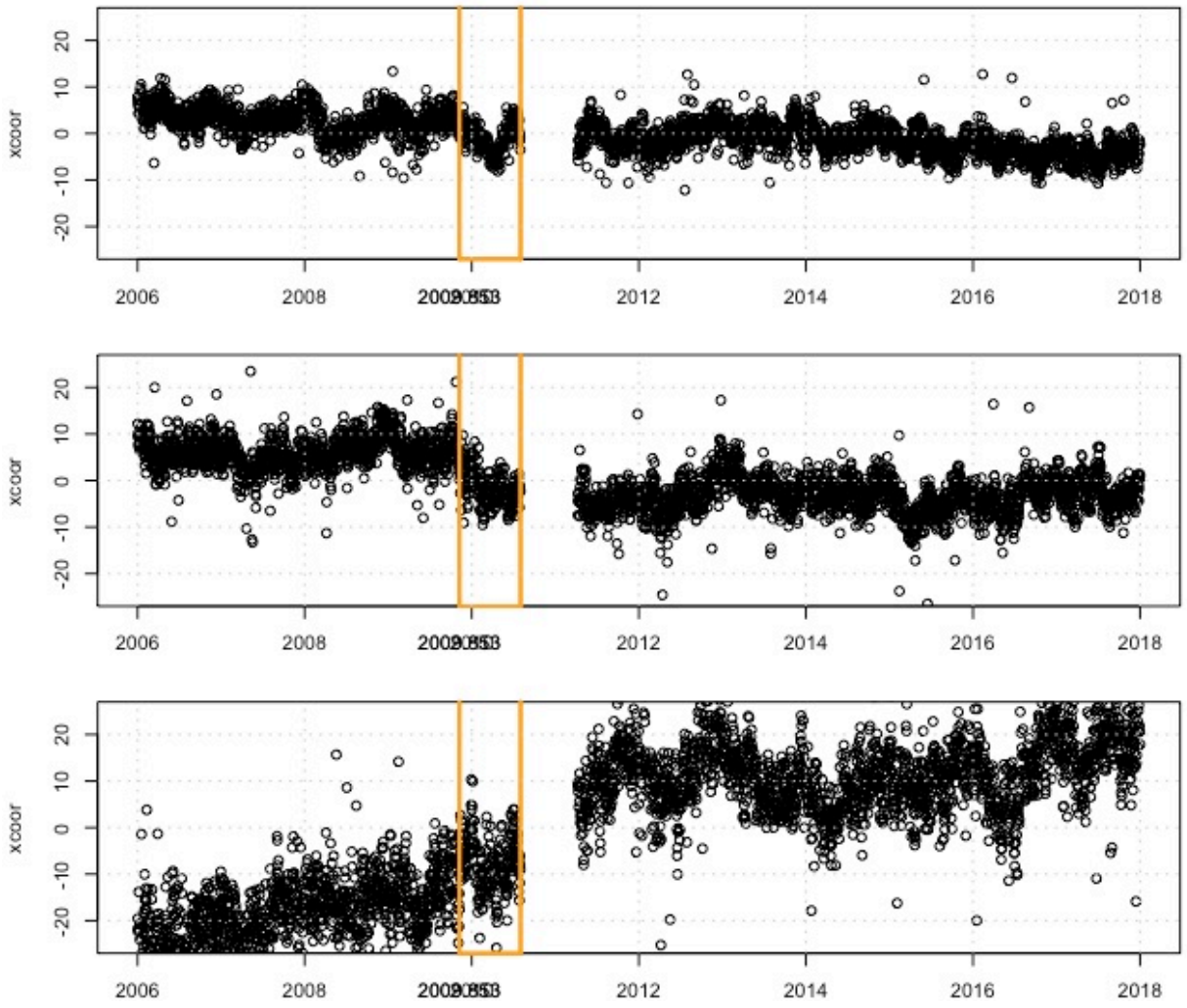

Station RU05

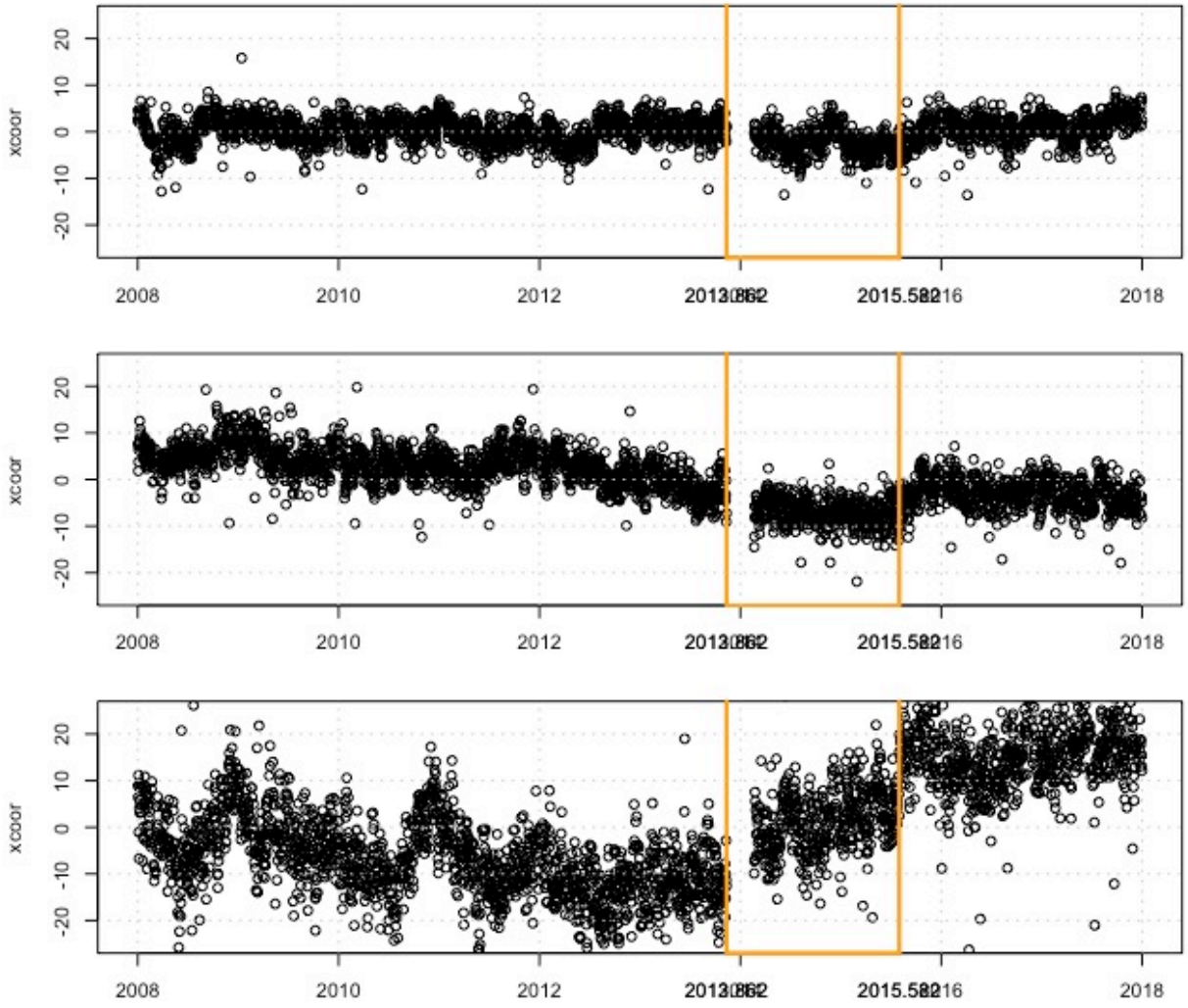

Station RU06

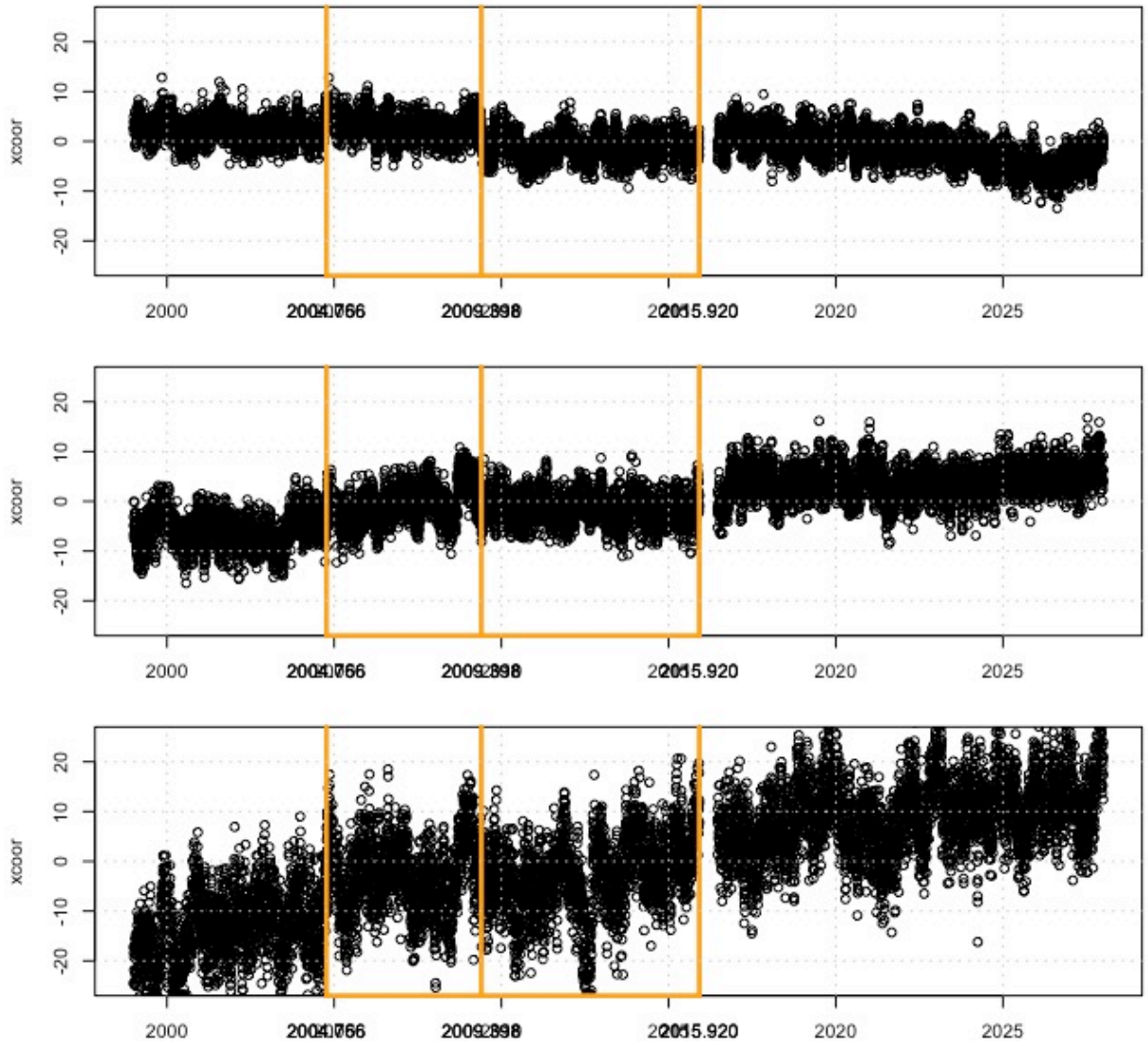

Station RU07

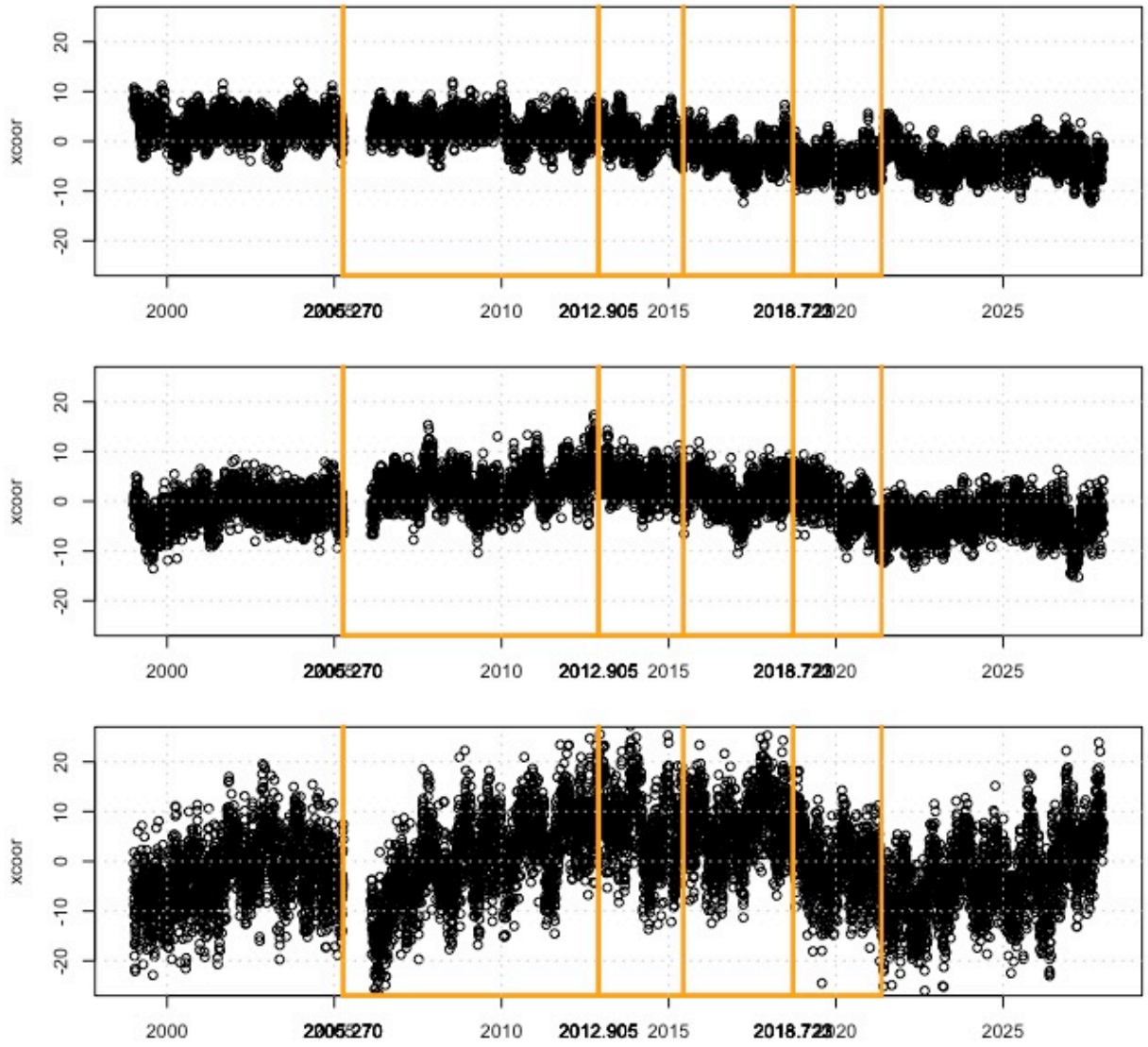

Station SU01

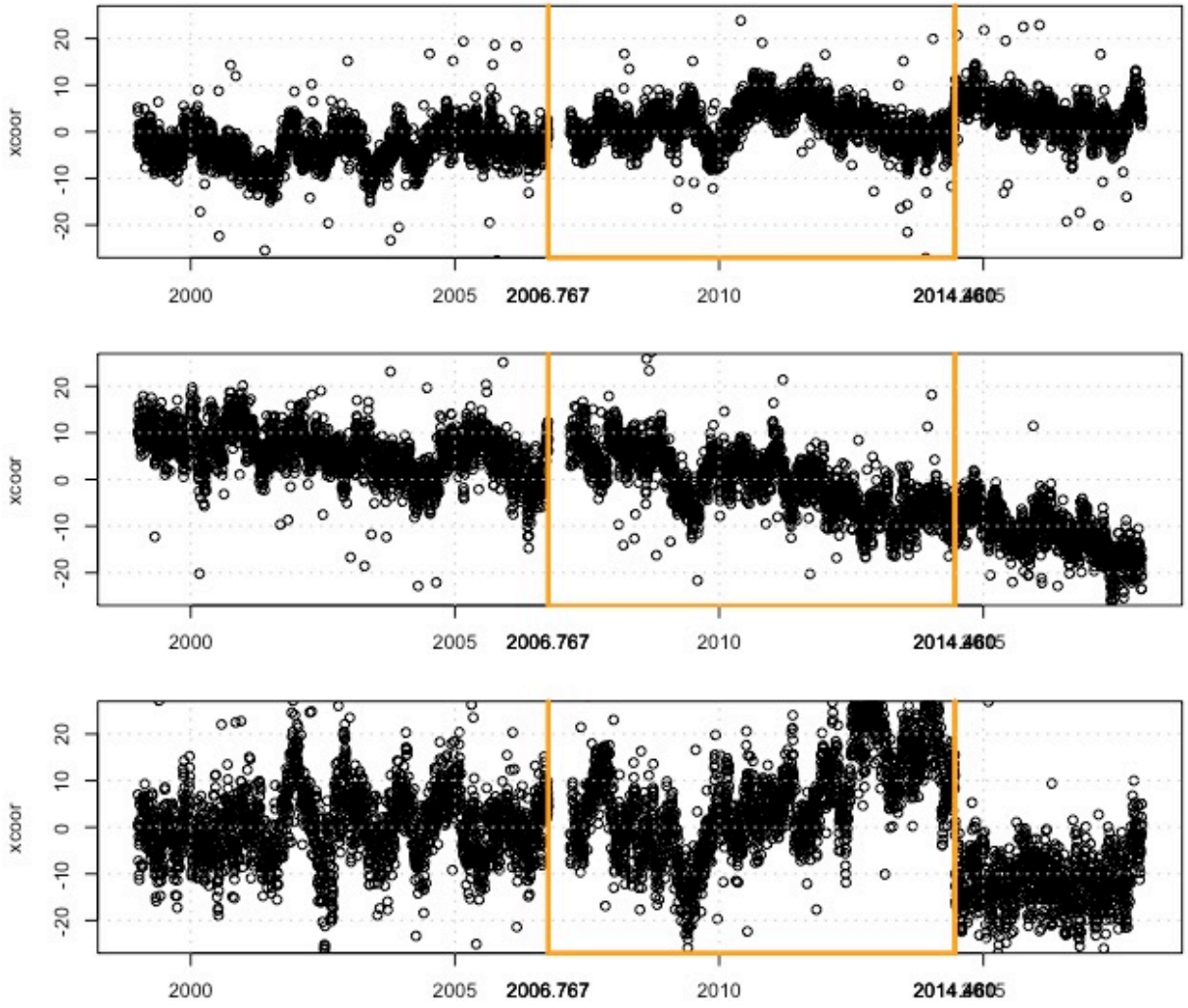

Station SU02

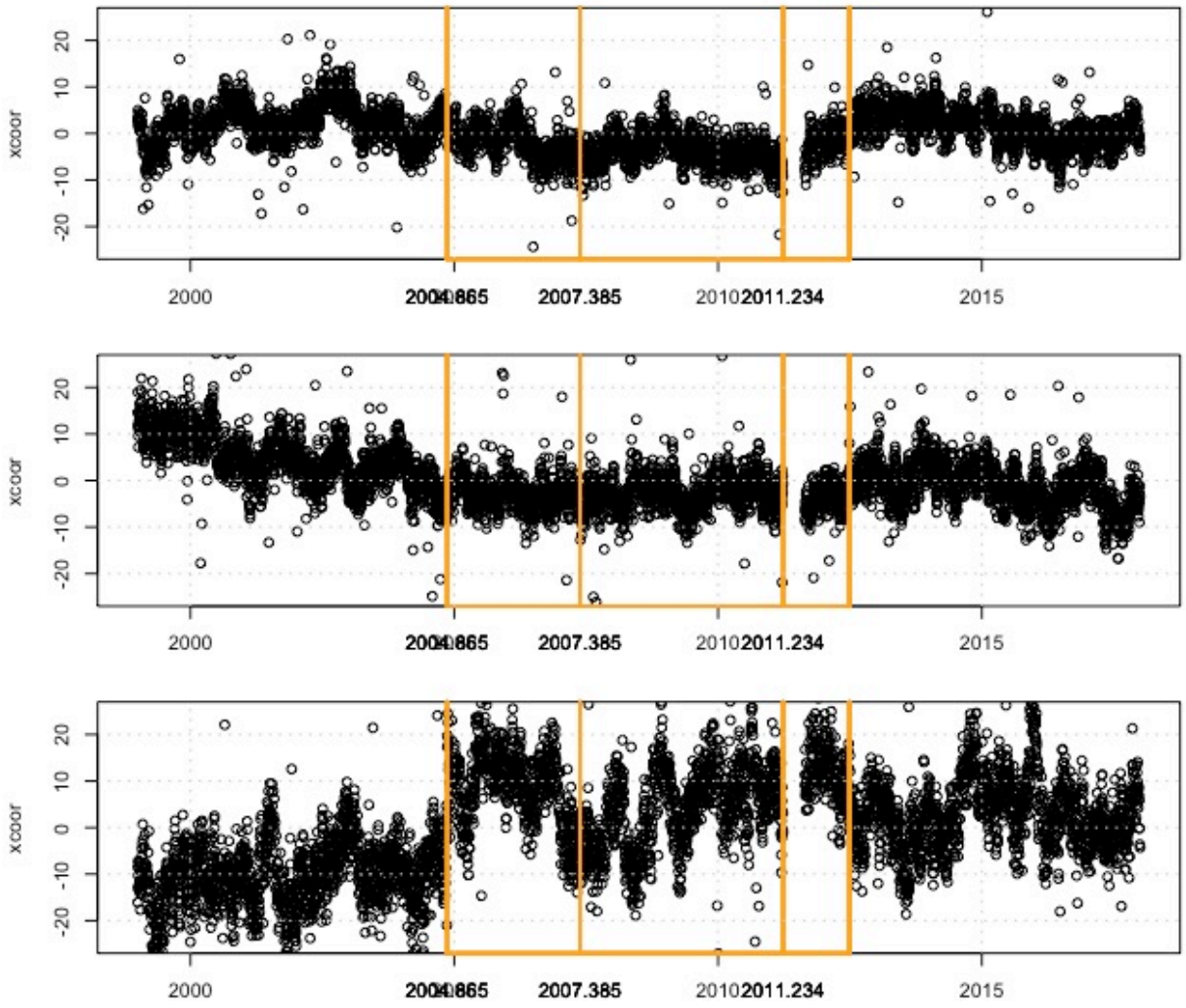

Station SU03

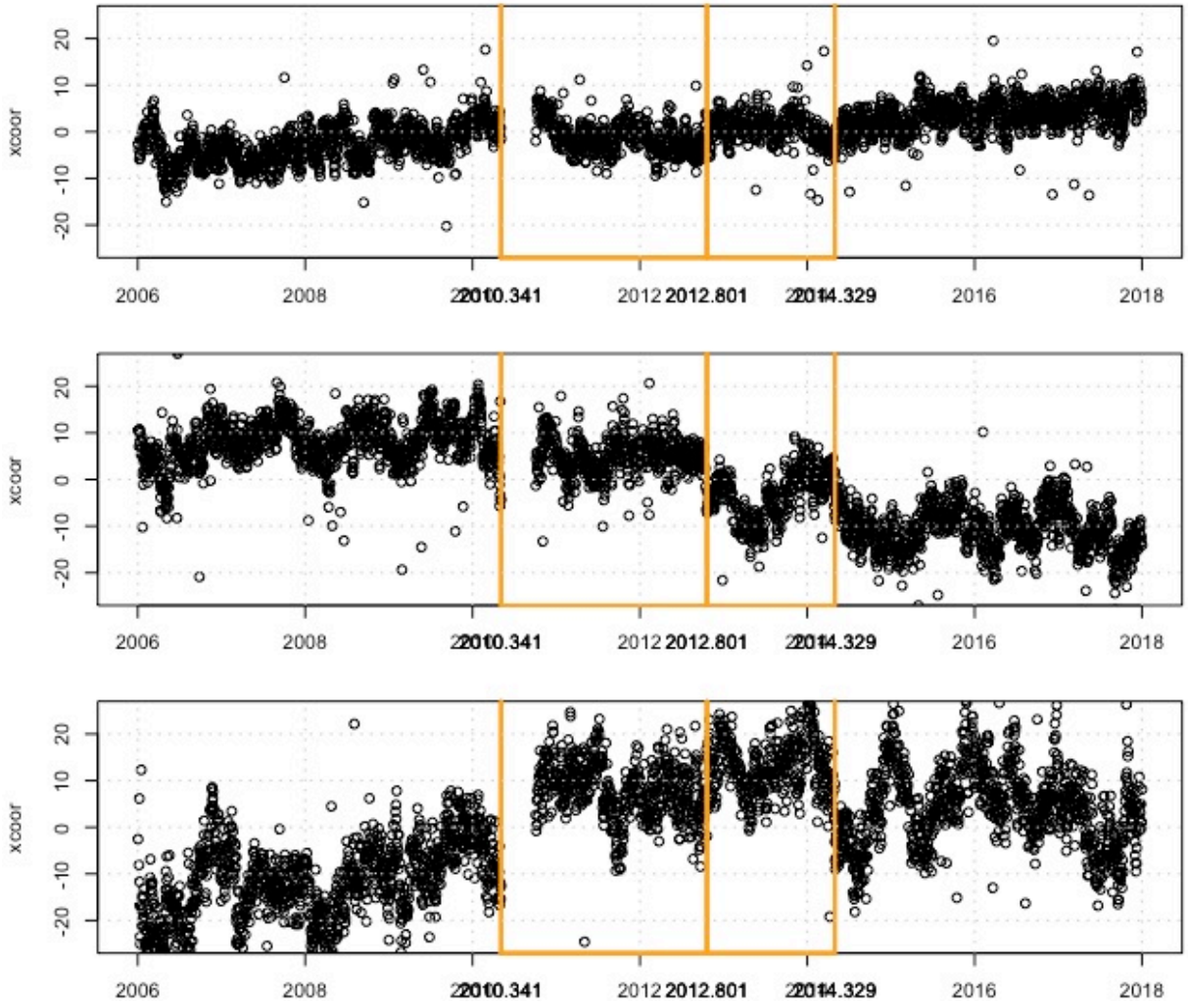

Station SU04

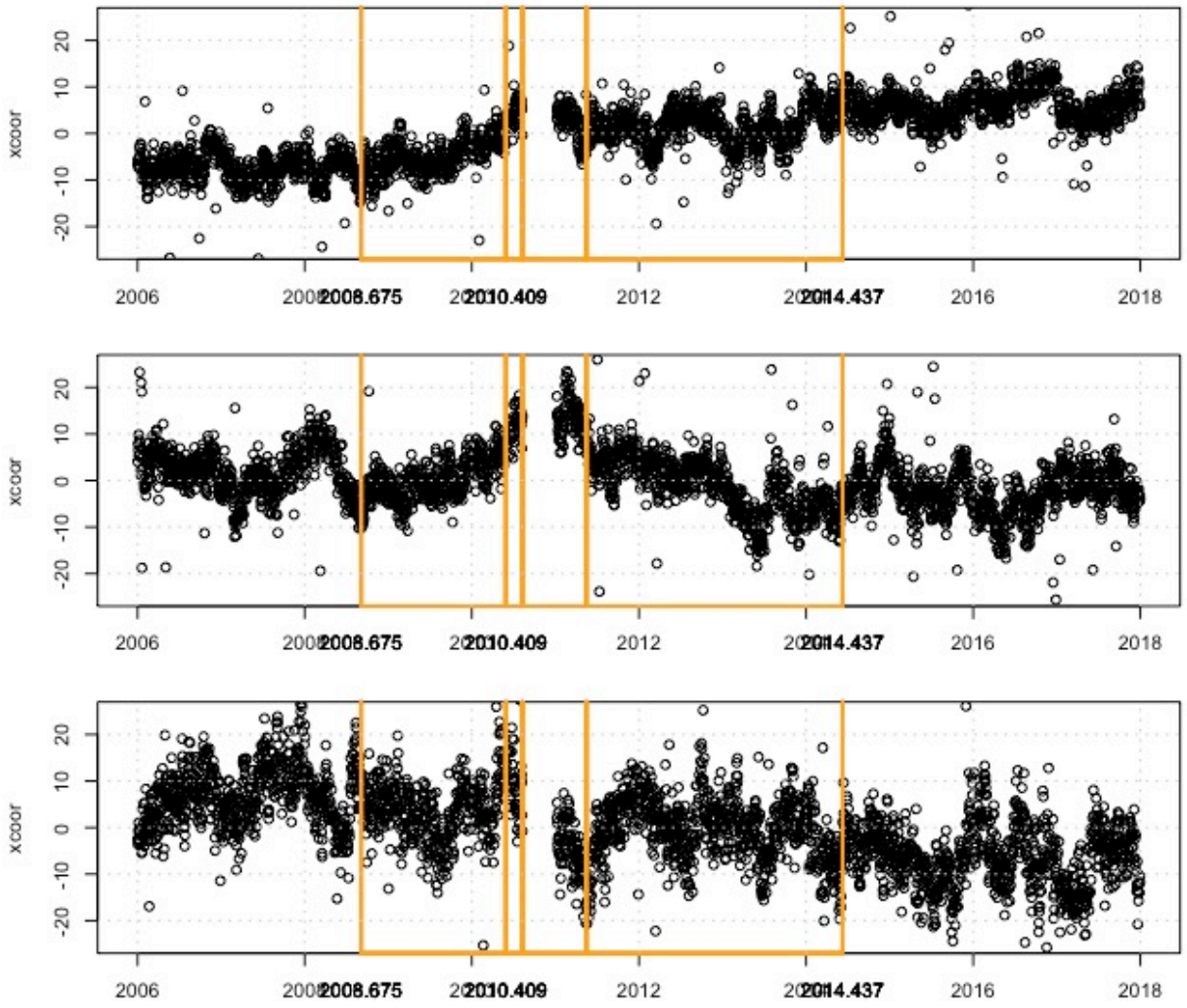

Station SU05

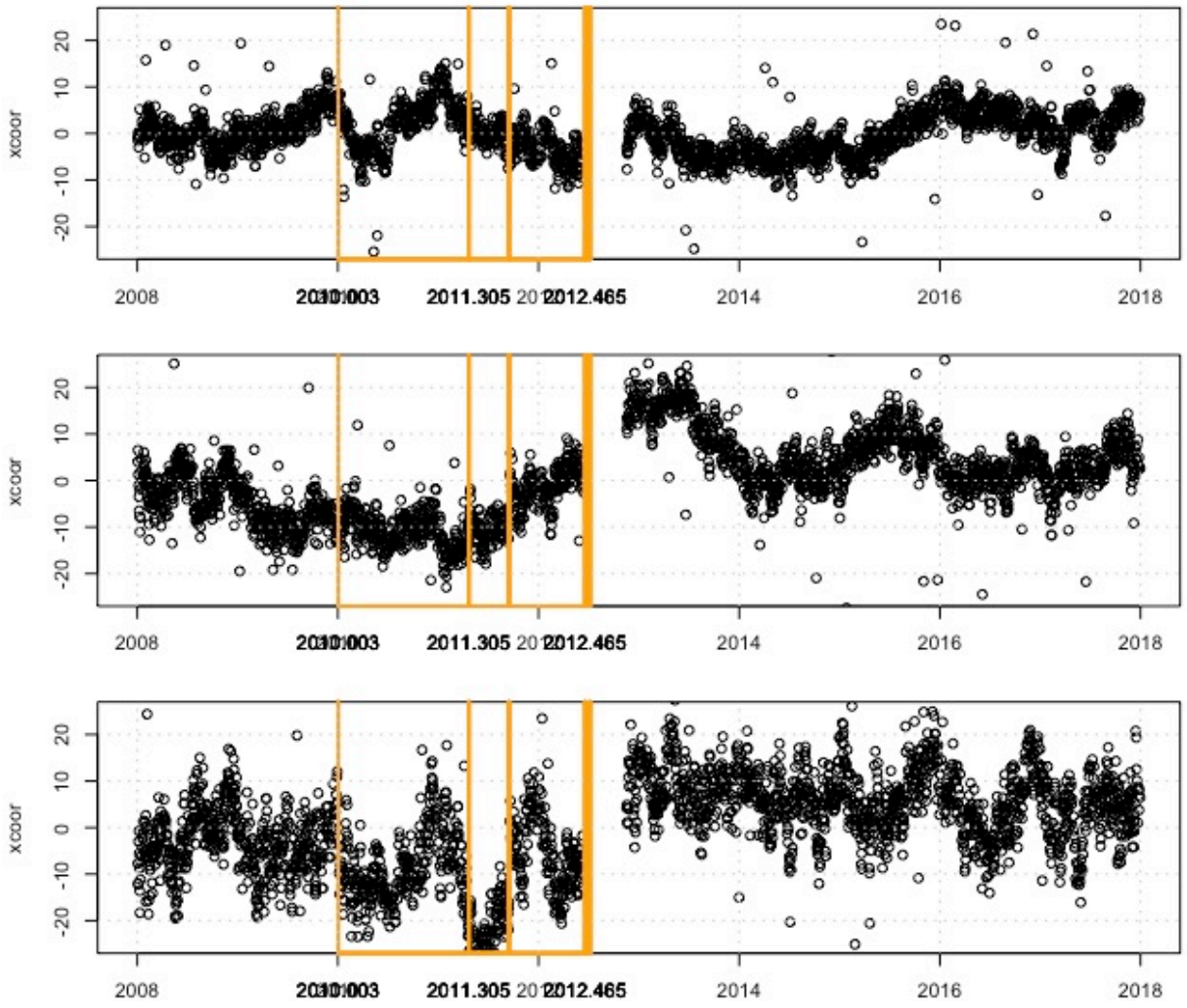

Station SU06

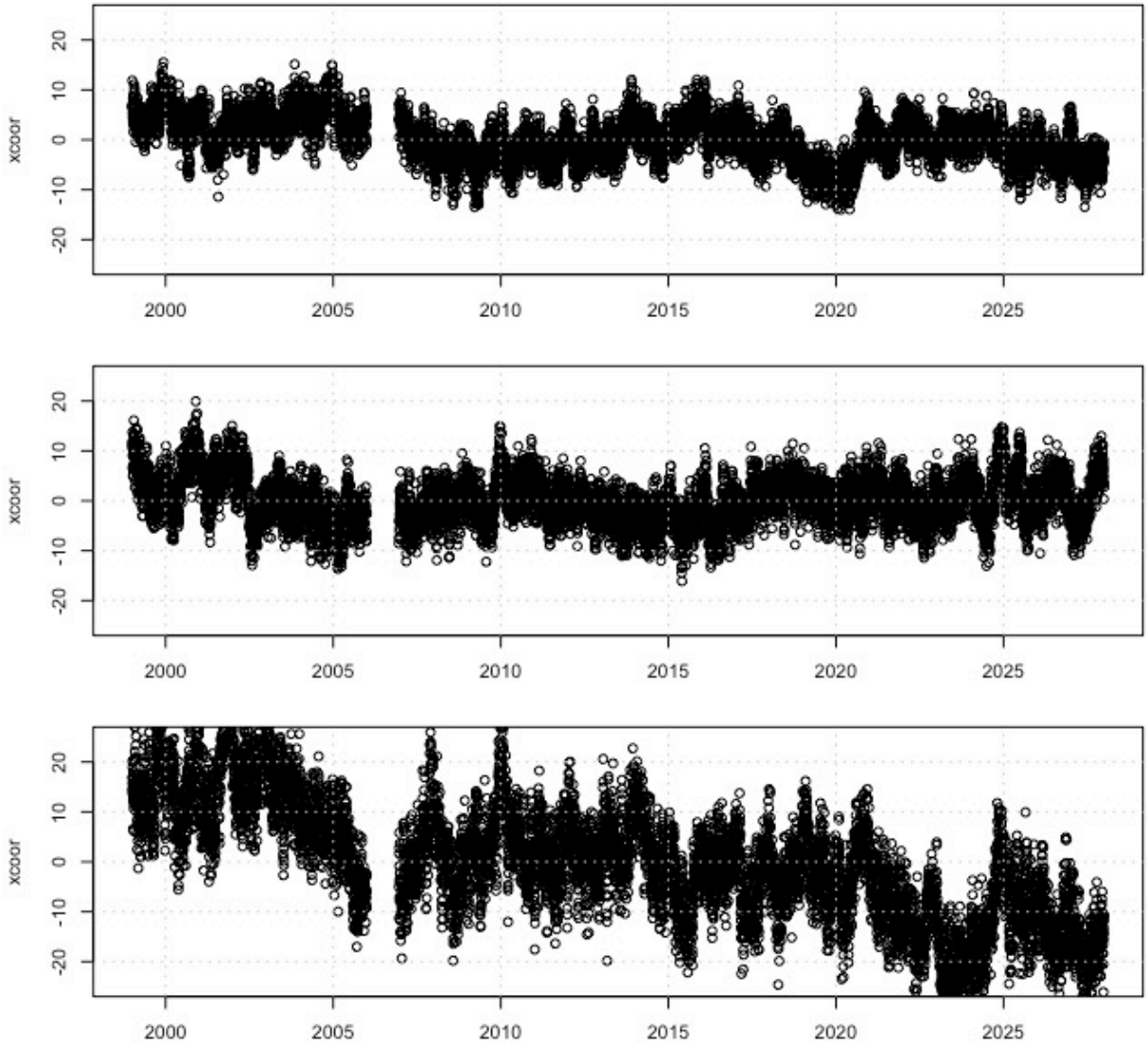

Station SU07

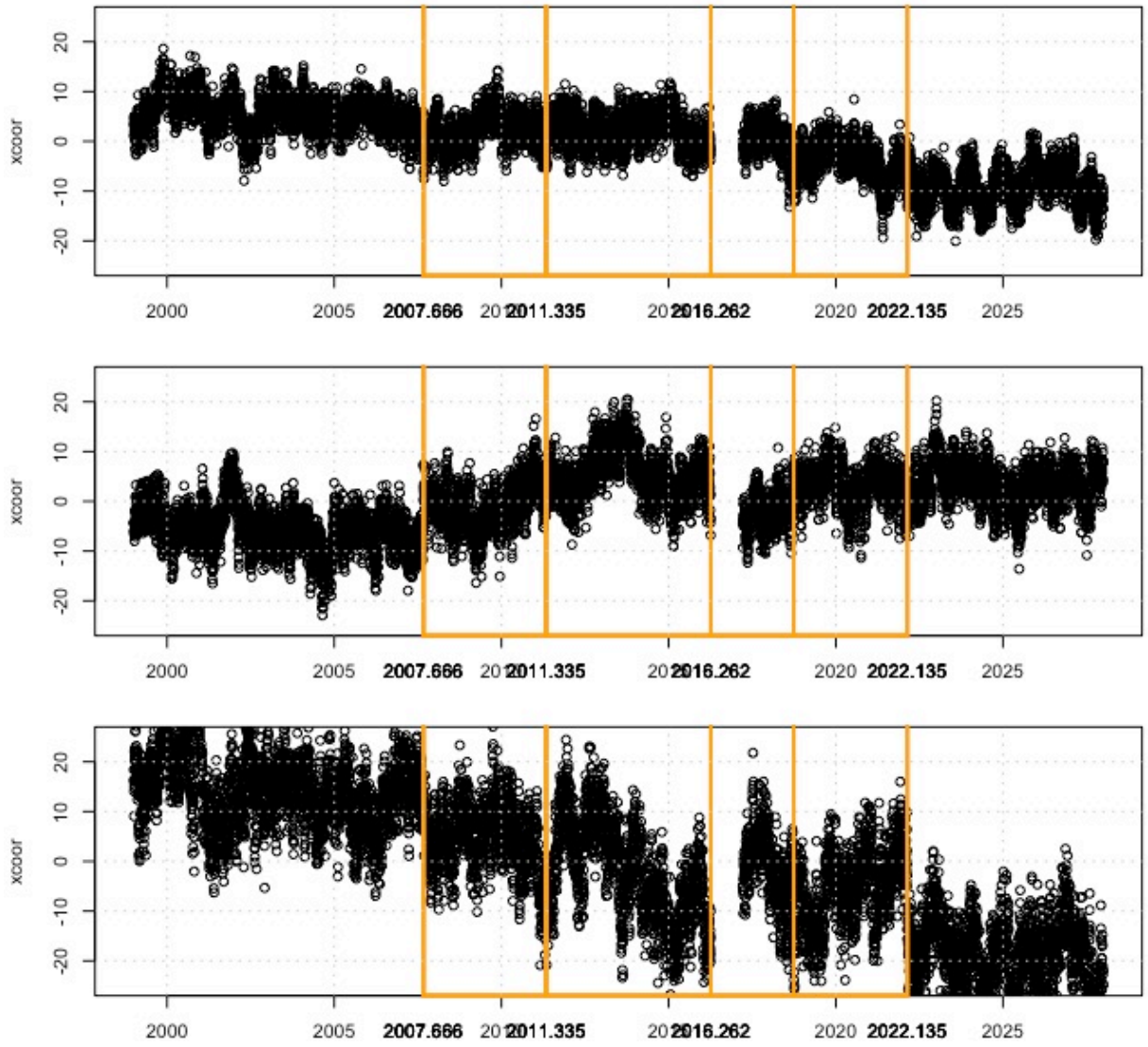

Appendix 2. Solution summary figures

Each figure shows a summary for the individual solution (S1–S9) and the average (S10). For the North, East and Vertical components (N, E, U), the estimated velocities and their 95% confidence intervals (two standard errors) are shown relative to the true velocities. Numbers above the graphs are the median of the velocity bias absolute values (dV_{50}) per quality group and for all stations. The bottom-right graph shows the ratios of velocity biases (dV) over their standard errors (s). The numbers above indicate the percentage of ratios inferior to 2 and the means of the ratios (N, E, and U components).

Solution S1

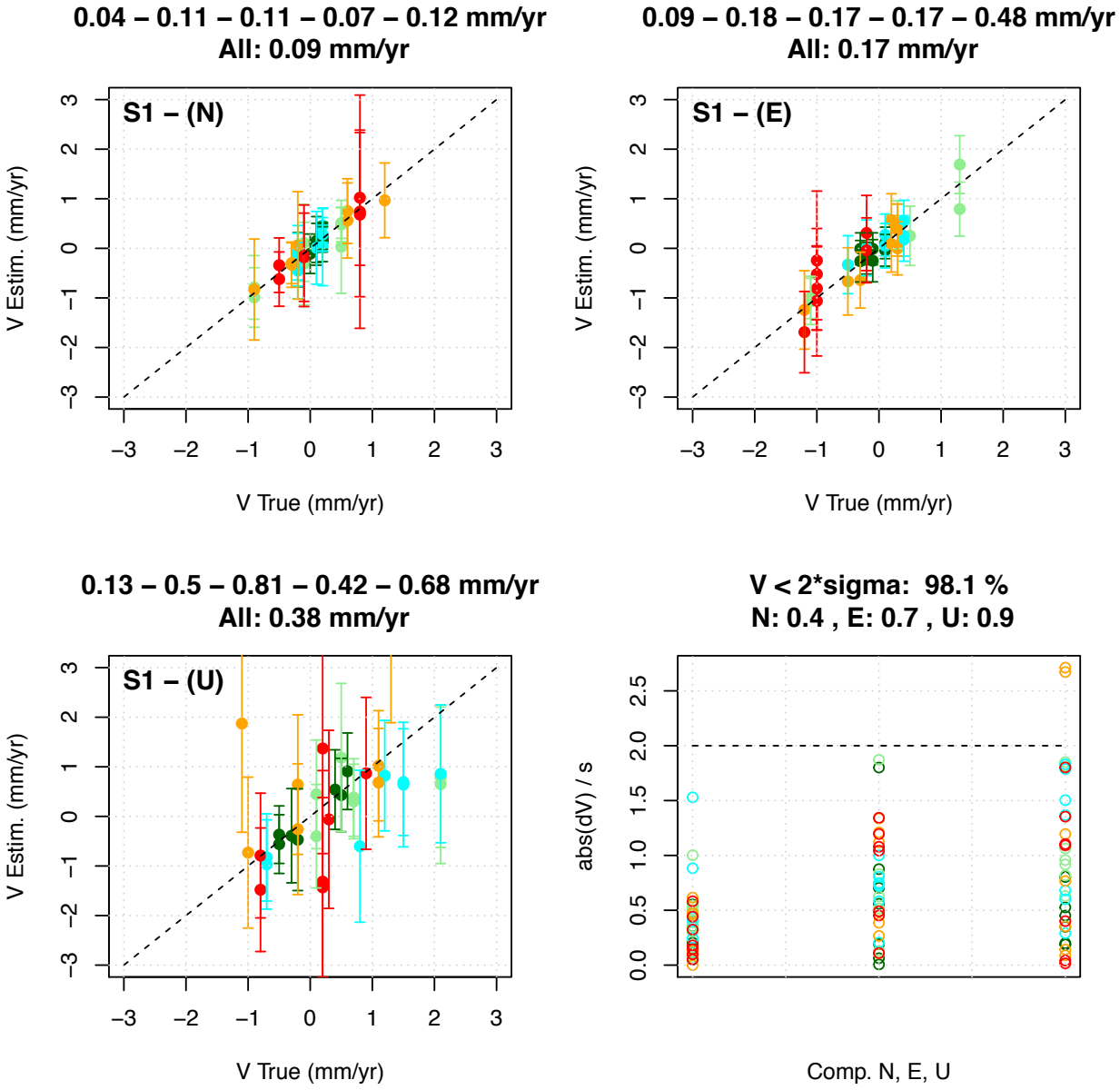

Solution S2

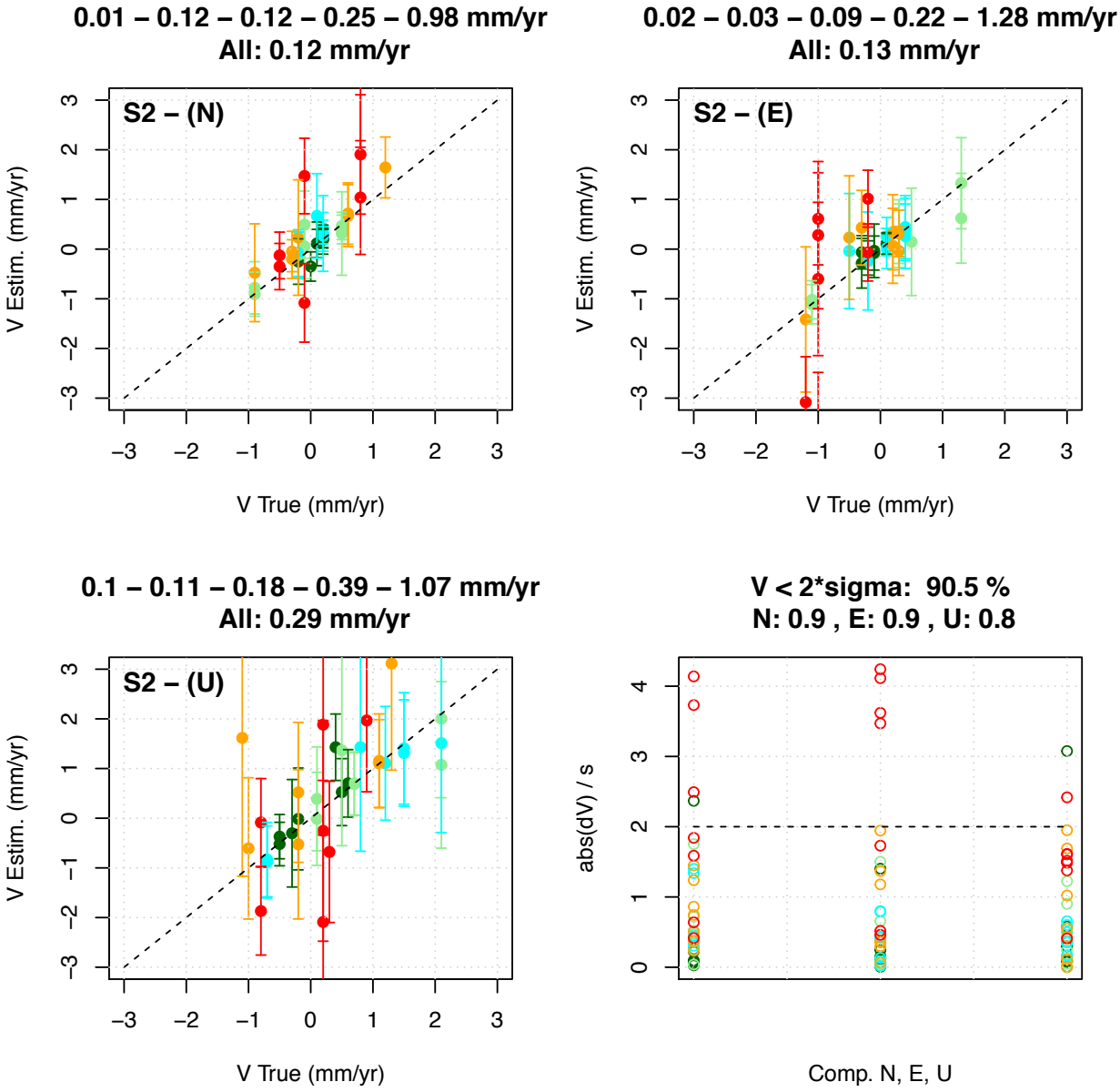
0.01 – 0.12 – 0.12 – 0.25 – 0.98 mm/yr
All: 0.12 mm/yr
S2 – (N)
V Estim. (mm/yr)
V True (mm/yr)
0.02 – 0.03 – 0.09 – 0.22 – 1.28 mm/yr
All: 0.13 mm/yr
S2 – (E)
V Estim. (mm/yr)
V True (mm/yr)
0.1 – 0.11 – 0.18 – 0.39 – 1.07 mm/yr
All: 0.29 mm/yr
S2 – (U)
V Estim. (mm/yr)
V True (mm/yr)
V < 2*sigma: 90.5 %
N: 0.9 , E: 0.9 , U: 0.8
abs(dV) / s
Comp. N, E, U

Solution S3

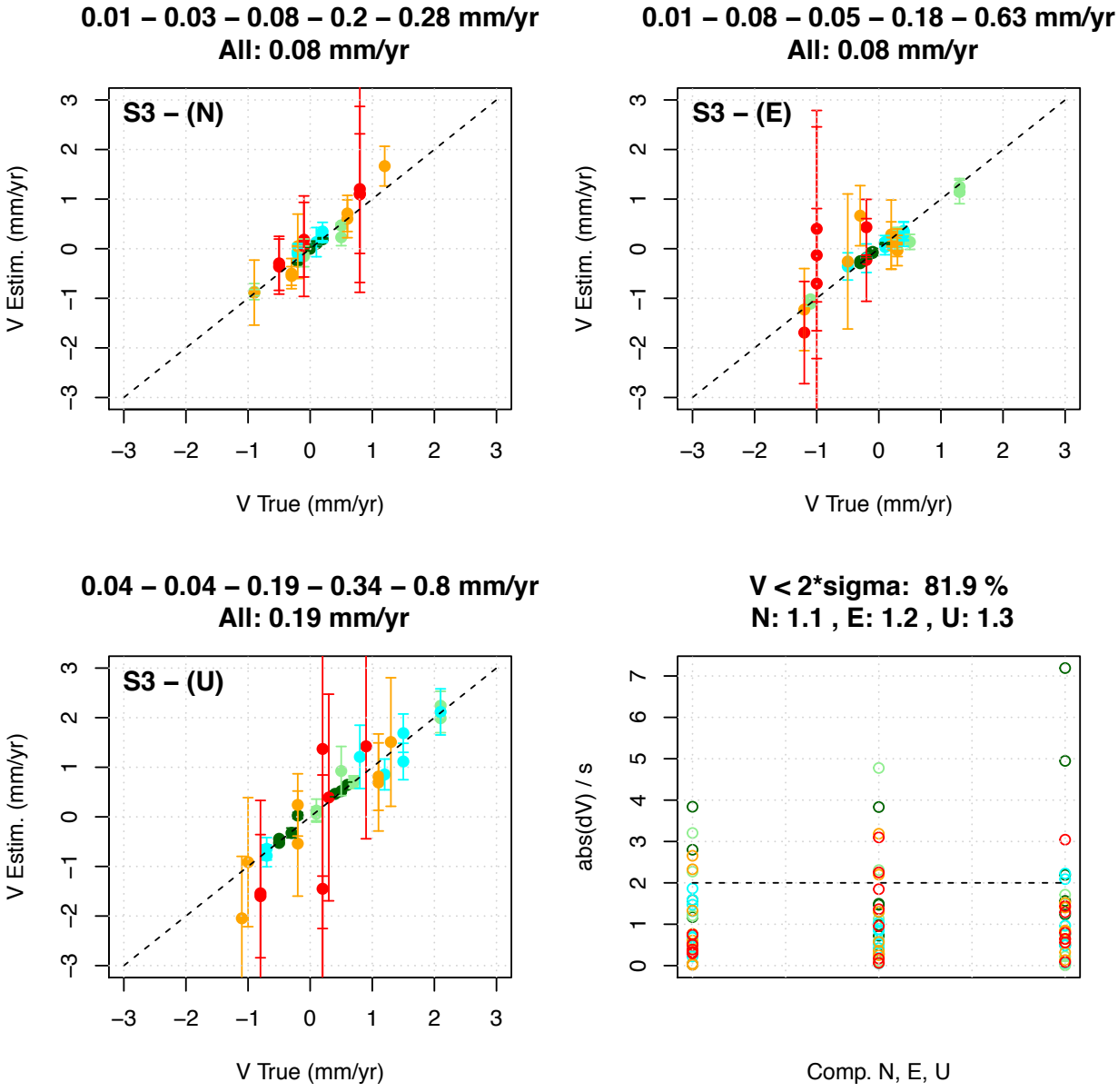
0.01 – 0.03 – 0.08 – 0.2 – 0.28 mm/yr
All: 0.08 mm/yr
S3 – (N)
V Estim. (mm/yr)
V True (mm/yr)
0.01 – 0.08 – 0.05 – 0.18 – 0.63 mm/yr
All: 0.08 mm/yr
S3 – (E)
V Estim. (mm/yr)
V True (mm/yr)
0.04 – 0.04 – 0.19 – 0.34 – 0.8 mm/yr
All: 0.19 mm/yr
S3 – (U)
V Estim. (mm/yr)
V True (mm/yr)
V < 2*sigma: 81.9 %
N: 1.1 , E: 1.2 , U: 1.3
abs(dV) / s
Comp. N, E, U

Solution S4

0.01 – 0.06 – 0.08 – 0.15 – 0.17 mm/yr
All: 0.08 mm/yr

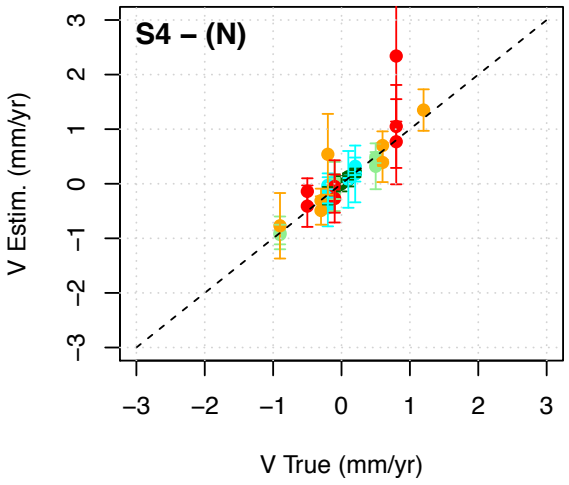

0.02 – 0.11 – 0.11 – 0.14 – 0.53 mm/yr
All: 0.1 mm/yr

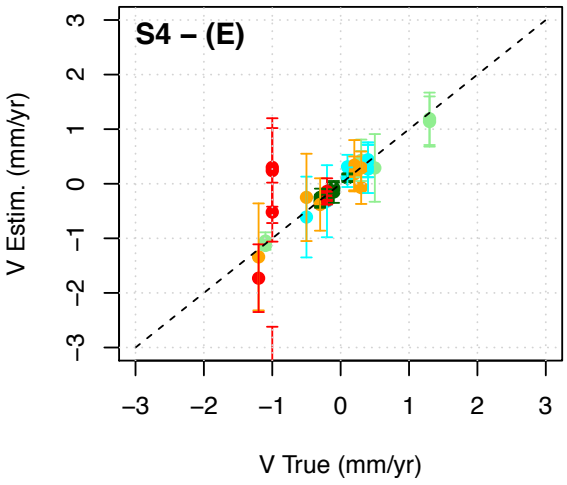

0.1 – 0.21 – 0.12 – 0.18 – 0.45 mm/yr
All: 0.15 mm/yr

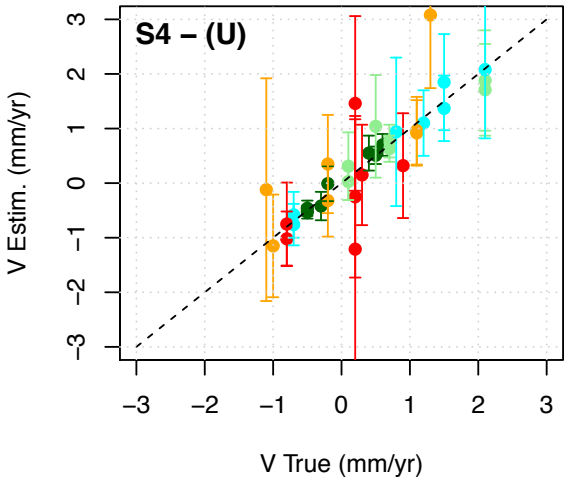

V < 2*sigma: 91.4 %
N: 0.8 , E: 29.5 , U: 0.7

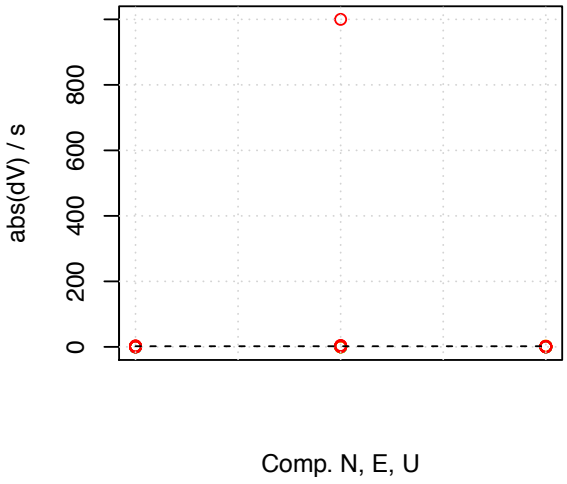

Solution S5

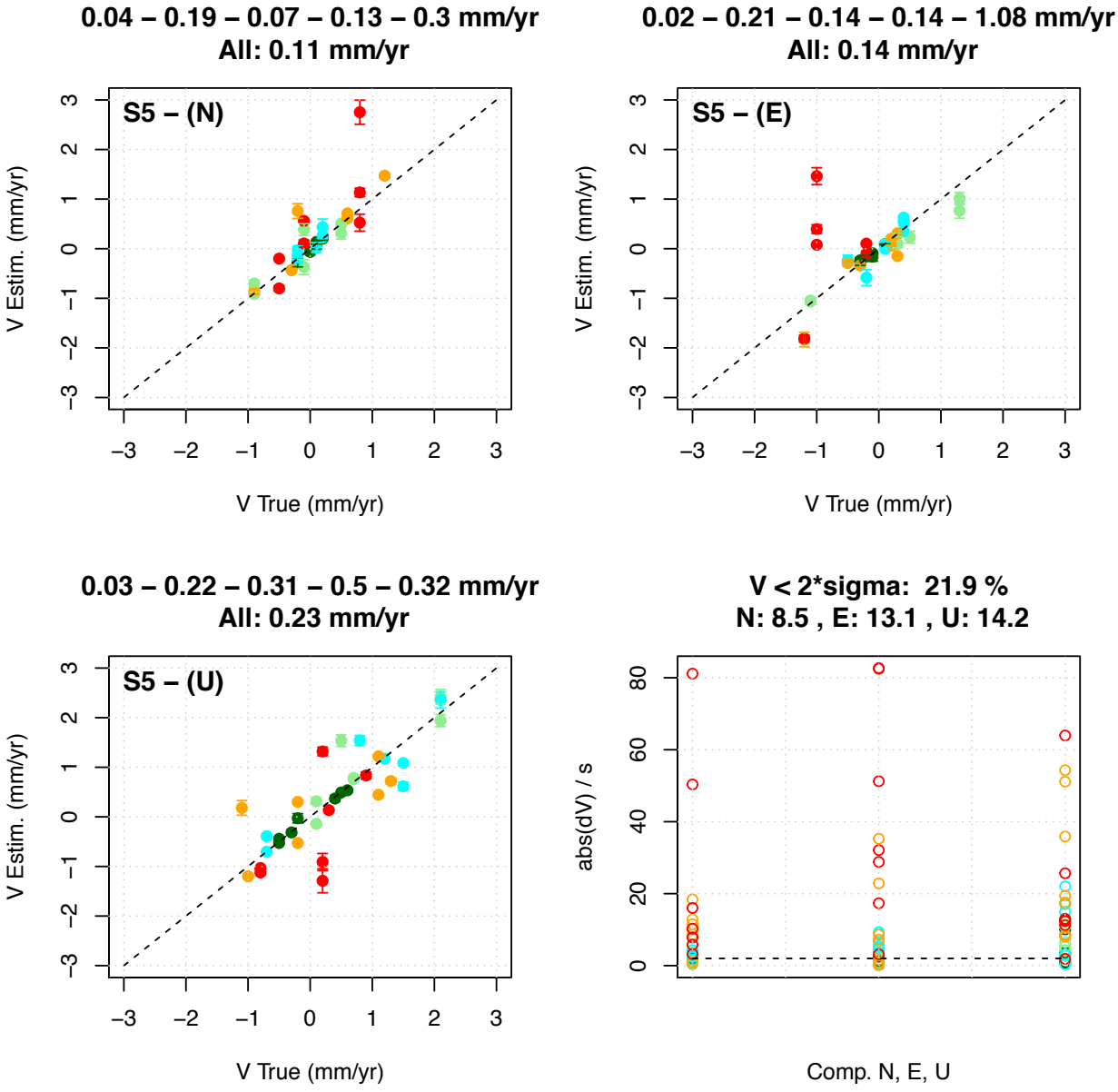
0.04 – 0.19 – 0.07 – 0.13 – 0.3 mm/yr
All: 0.11 mm/yr
S5 – (N)
V Estim. (mm/yr)
V True (mm/yr)
0.02 – 0.21 – 0.14 – 0.14 – 1.08 mm/yr
All: 0.14 mm/yr
S5 – (E)
V Estim. (mm/yr)
V True (mm/yr)
0.03 – 0.22 – 0.31 – 0.5 – 0.32 mm/yr
All: 0.23 mm/yr
S5 – (U)
V Estim. (mm/yr)
V True (mm/yr)
V < 2*sigma: 21.9 %
N: 8.5 , E: 13.1 , U: 14.2
abs(dV) / s
Comp. N, E, U

Solution S6

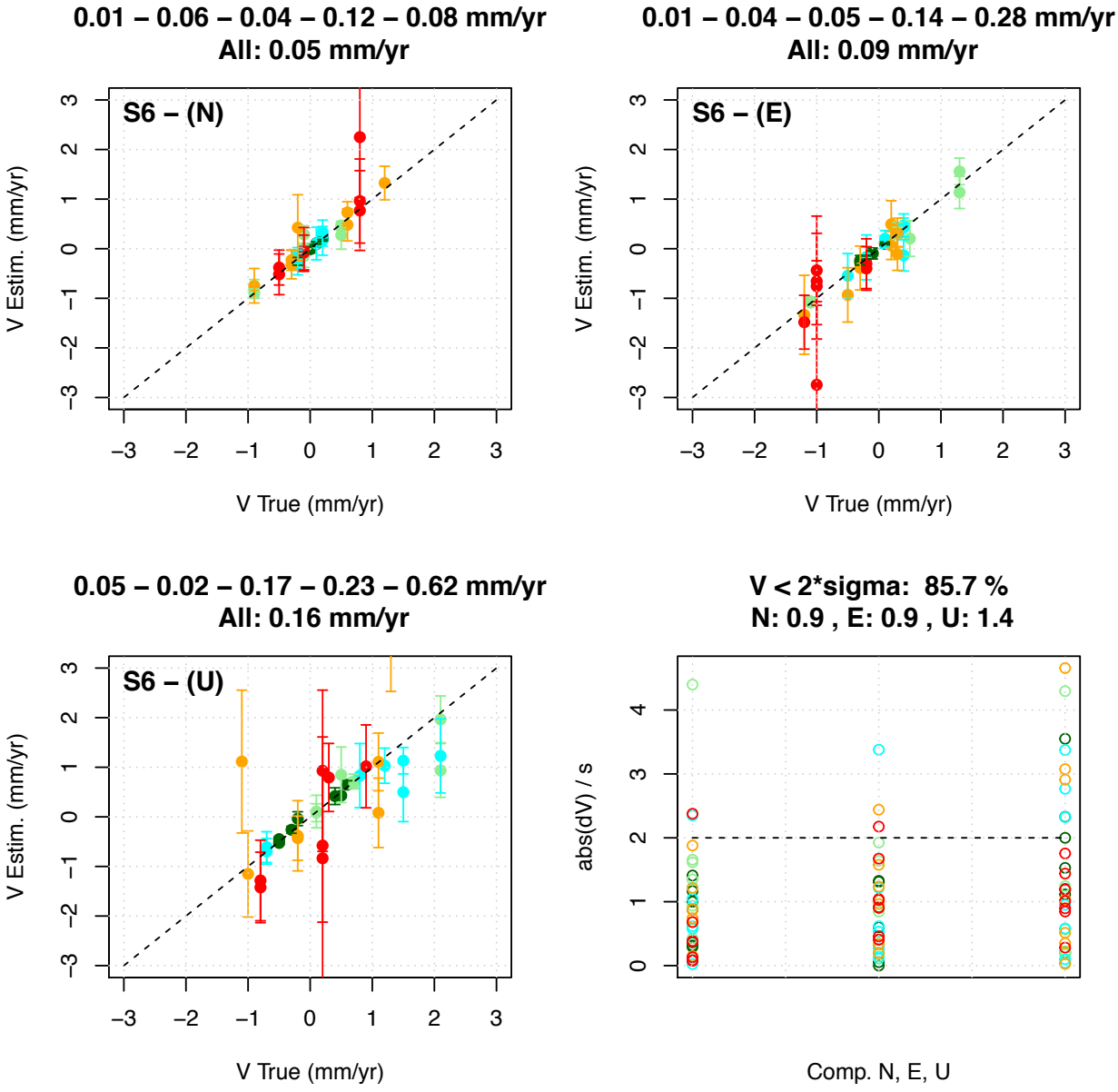
0.01 – 0.06 – 0.04 – 0.12 – 0.08 mm/yr
All: 0.05 mm/yr
S6 – (N)
V Estim. (mm/yr)
V True (mm/yr)
0.01 – 0.04 – 0.05 – 0.14 – 0.28 mm/yr
All: 0.09 mm/yr
S6 – (E)
V Estim. (mm/yr)
V True (mm/yr)
0.05 – 0.02 – 0.17 – 0.23 – 0.62 mm/yr
All: 0.16 mm/yr
S6 – (U)
V Estim. (mm/yr)
V True (mm/yr)
V < 2*sigma: 85.7 %
N: 0.9 , E: 0.9 , U: 1.4
abs(dV) / s
Comp. N, E, U

Solution S7

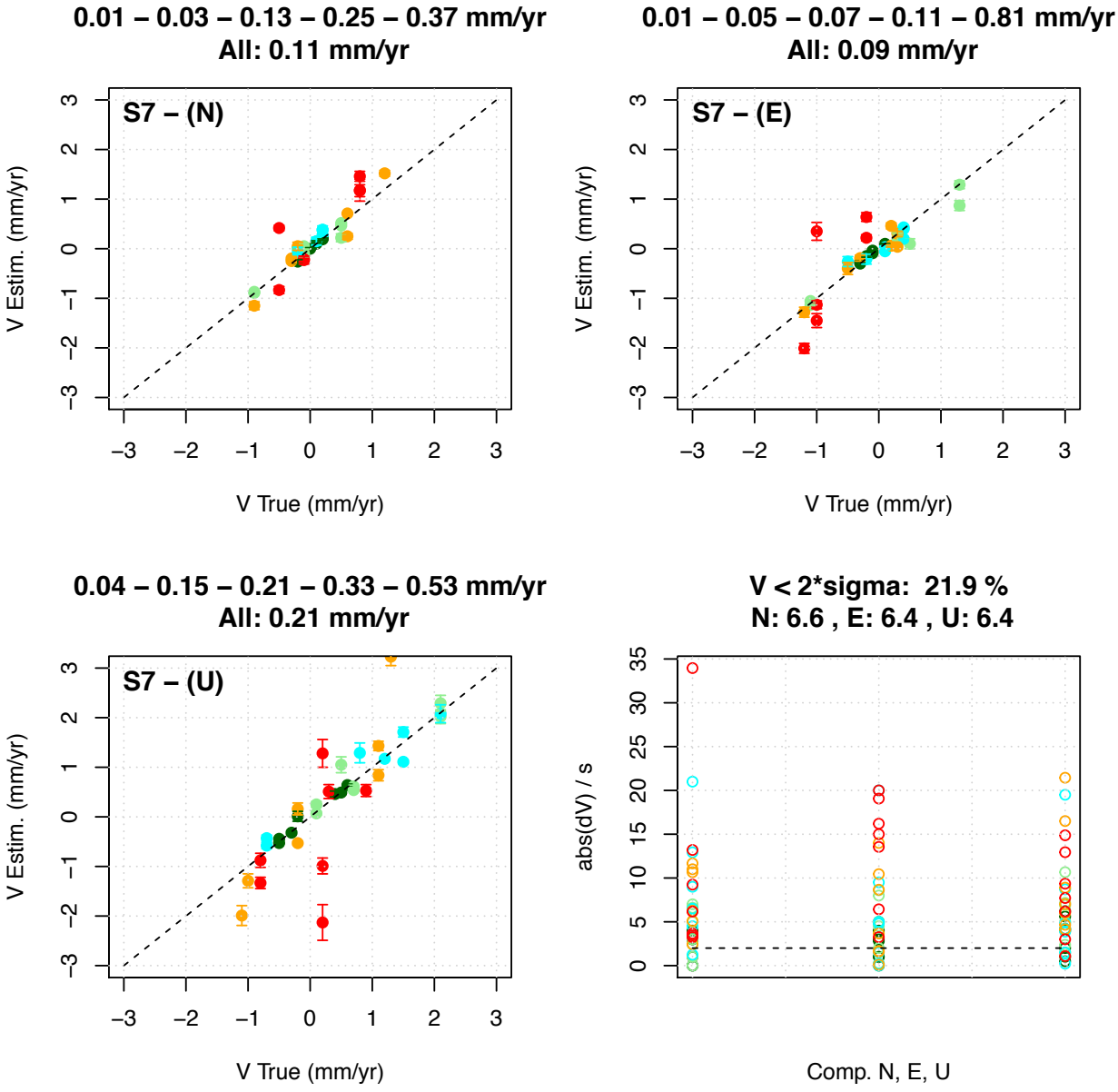
0.01 – 0.03 – 0.13 – 0.25 – 0.37 mm/yr
All: 0.11 mm/yr
S7 – (N)
V Estim. (mm/yr)
V True (mm/yr)
0.01 – 0.05 – 0.07 – 0.11 – 0.81 mm/yr
All: 0.09 mm/yr
S7 – (E)
V Estim. (mm/yr)
V True (mm/yr)
0.04 – 0.15 – 0.21 – 0.33 – 0.53 mm/yr
All: 0.21 mm/yr
S7 – (U)
V Estim. (mm/yr)
V True (mm/yr)
V < 2*sigma: 21.9 %
N: 6.6 , E: 6.4 , U: 6.4
abs(dV) / s
Comp. N, E, U

Solution S8

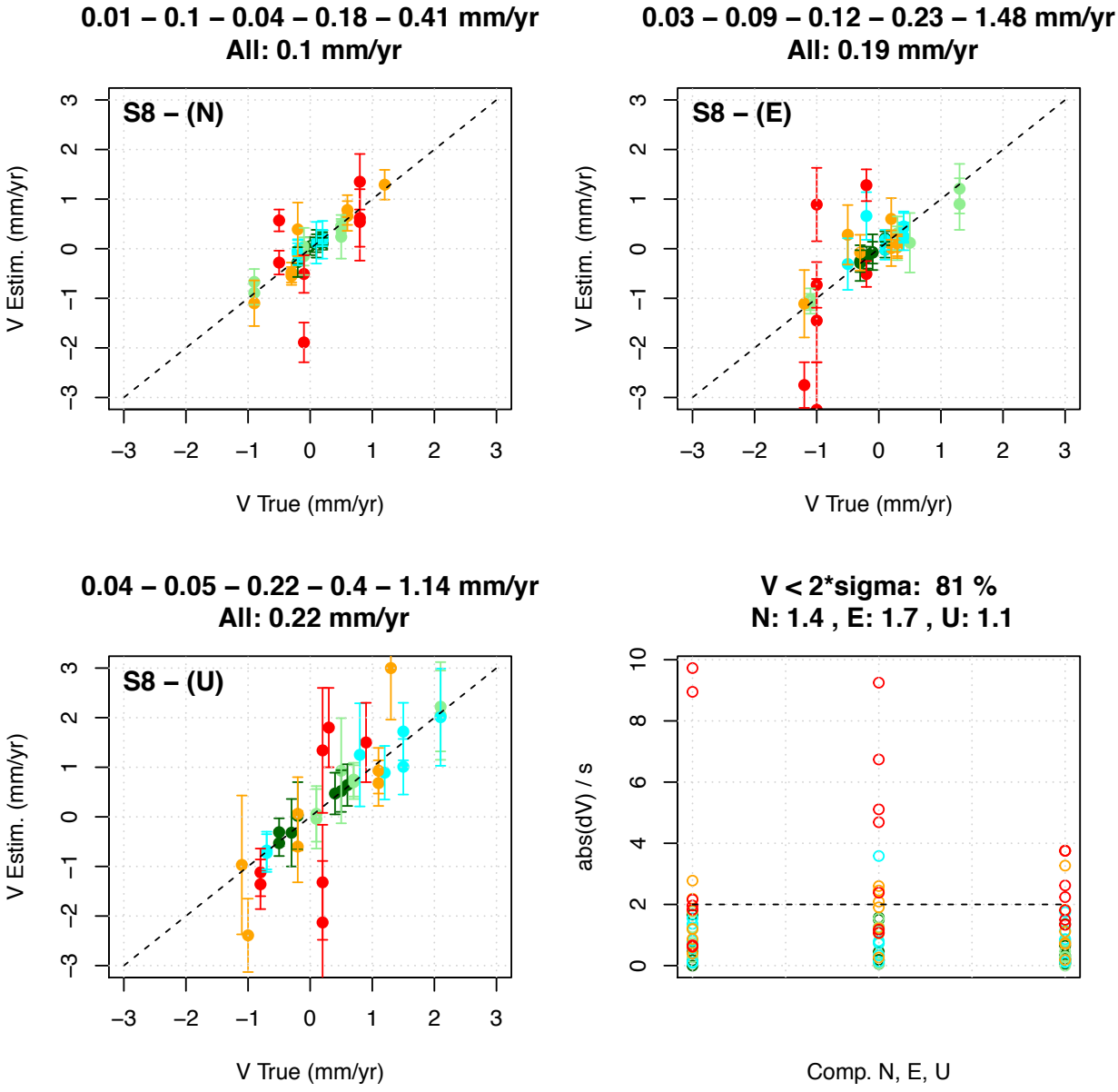
0.01 – 0.1 – 0.04 – 0.18 – 0.41 mm/yr
All: 0.1 mm/yr
S8 – (N)
V Estim. (mm/yr)
V True (mm/yr)
0.03 – 0.09 – 0.12 – 0.23 – 1.48 mm/yr
All: 0.19 mm/yr
S8 – (E)
V Estim. (mm/yr)
V True (mm/yr)
0.04 – 0.05 – 0.22 – 0.4 – 1.14 mm/yr
All: 0.22 mm/yr
S8 – (U)
V Estim. (mm/yr)
V True (mm/yr)
V < 2*sigma: 81 %
N: 1.4 , E: 1.7 , U: 1.1
abs(dV) / s
Comp. N, E, U

Solution S9

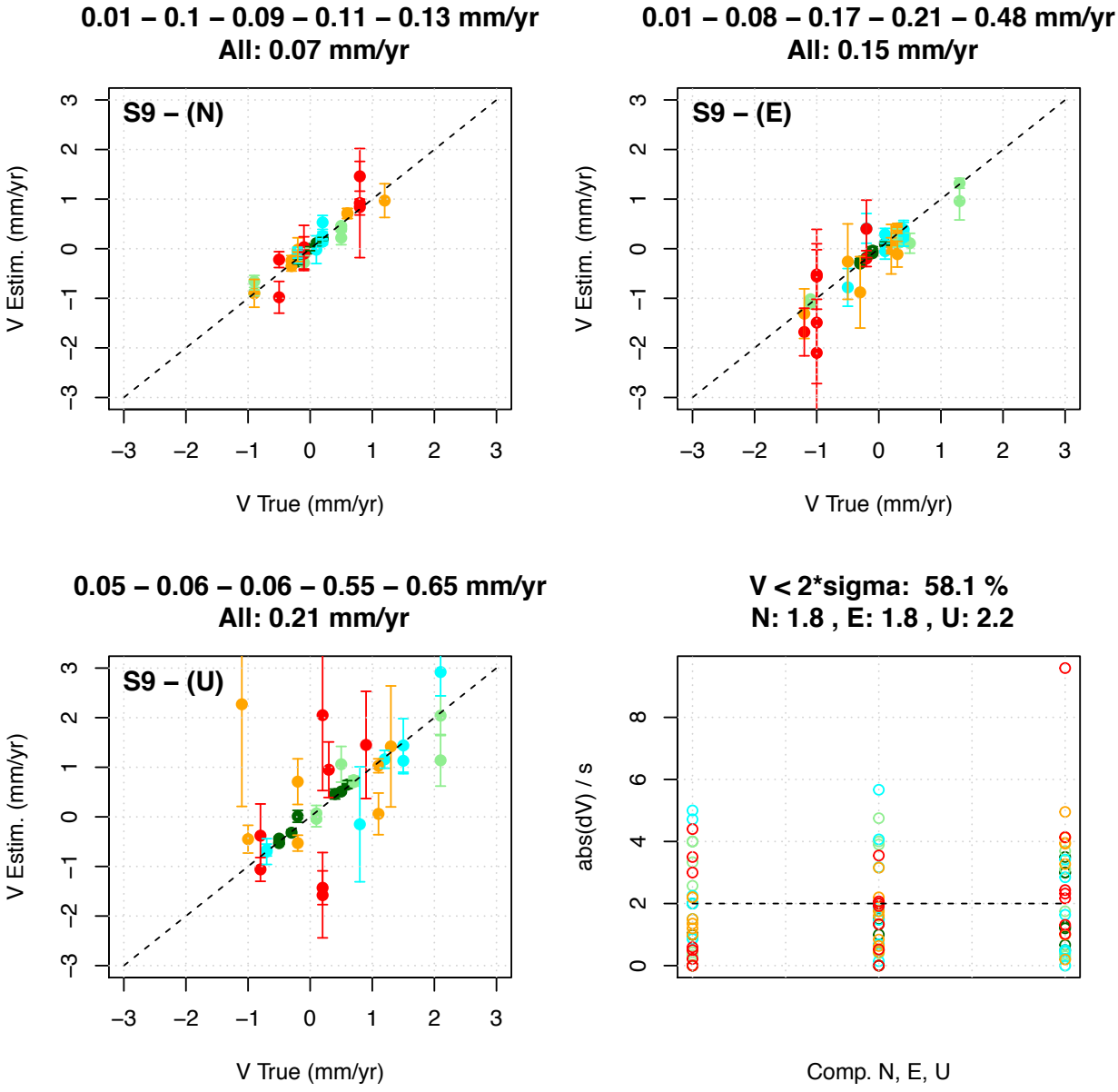
0.01 – 0.1 – 0.09 – 0.11 – 0.13 mm/yr
All: 0.07 mm/yr
S9 – (N)
V Estim. (mm/yr)
V True (mm/yr)
0.01 – 0.08 – 0.17 – 0.21 – 0.48 mm/yr
All: 0.15 mm/yr
S9 – (E)
V Estim. (mm/yr)
V True (mm/yr)
0.05 – 0.06 – 0.06 – 0.55 – 0.65 mm/yr
All: 0.21 mm/yr
S9 – (U)
V Estim. (mm/yr)
V True (mm/yr)
V < 2*sigma: 58.1 %
N: 1.8 , E: 1.8 , U: 2.2
abs(dV) / s
Comp. N, E, U

Solution S10 – unweighted average